Energetic particle physics and optimization methods for stellarators

Don Spong

Oak Ridge National Laboratory

Collaborators: Jacobo Varela, Steve Hirshman, Jeremy Lore, John Canik, Yasushi Todo, K. Ogawa, K. Toi, Axel Könies, A. Melnikov, S. Sharapov

The Hangzhou International Stellarator Workshop (HISW2018)

March 26-28, 2018

Zhejiang University

Hangzhou, China

Work supported by U.S. Department of Energy, Office of Science under DE-FC02-04ER54698, DE-AC52-07NA27344, DE-FG02-07ER54917, DE-SC00-16268, and DE-AC05-00OR22725

ORNL is managed by UT-Battelle
for the US Department of Energy

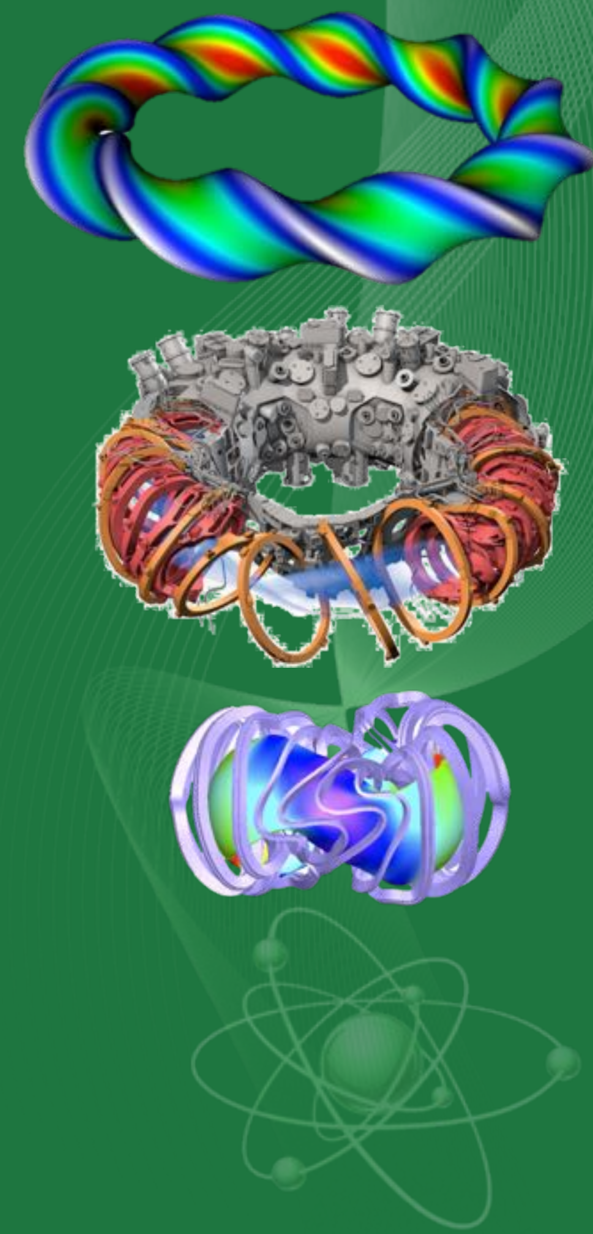

Energetic particle (EP) transport in stellarators

- Energetic particle confinement: remains important question for existing and future 3D systems
  - Heating efficiency, ignition margin, PFC damage
  - Very difficult to achieve good alpha particle confinement for stellarator reactors – not at tokamak levels yet
- EP confinement improvement examples
  - LHD inward shifted discharges
  - J-optimization, QO systems
  - Large aspect ratio IPP designs
  - NCSX design and ARIES-CS study
- Should consider both classical and turbulent losses

EP loss channels → *Classical orbit loss*

EP loss channels → *Instability-induced loss (Alfvén modes)*

OAK RIDGE
National Laboratory

Outline

- Introduction
  - Stellarator optimization
  - Confinement optimization targets
- **Energetic particle confinement**
- **Energetic particle stability**

Synthesis of 3D configurations

- Coils ➡ outer magnetic surface shape ➡ physics properties
- 3D shapes open up very large design space: effectively ~ 40 independent parameters (A. Boozer, L. P Ku, 2010) based on SVD analysis
- Axisymmetric tokamak shape parameters: R_0/a, κ, δ
- Thought experiment: quantize shape parameters into 10 levels
  - 10^3 2D configurations vs. 10^{40} 3D configurations => “combinatorial explosion”
- STELLOPT:

Adjust plasma boundary or coil geometry shape → Solve 3D equilibrium → Calculate χ^2 (physics + engr. targets) → Levenberg-Marquardt or other method used to minimize χ^2 → Adjust plasma boundary or coil geometry shape

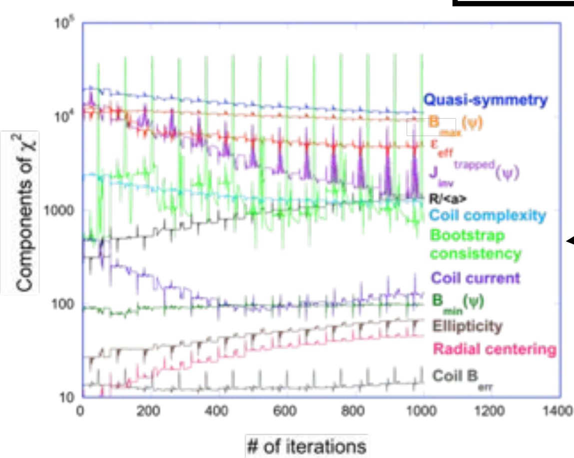

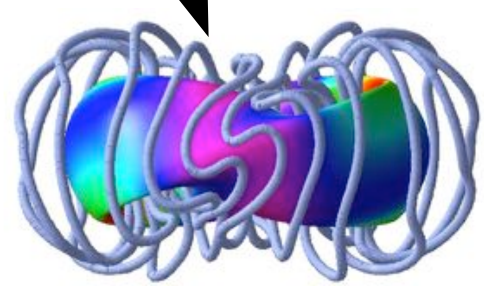

Orbit confinement has been a dominant factor in stellarator optimization

Closed helical contours

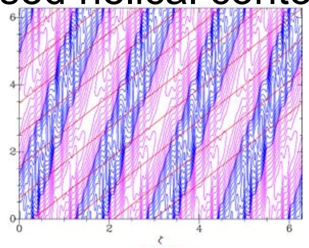

Closed toroidal contours

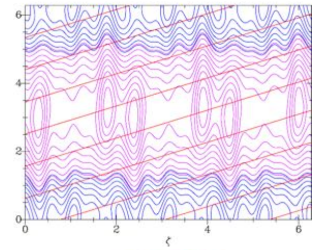

Closed poloidal contours

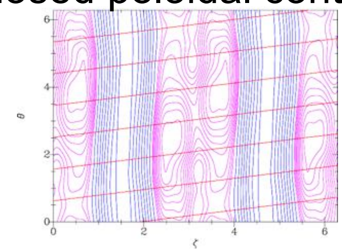

Examples:

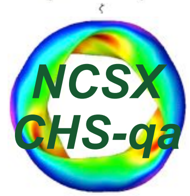

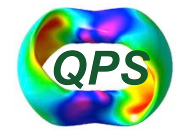

Heliotron-J

- Quasi-symmetry $B = B(\psi, M\Theta - N\zeta)$ Nührenberg (1988)
  - Ideal (but unachieved) goal $\quad \dfrac{(B \times \nabla\psi)\cdot\nabla B}{\vec{B}\cdot\nabla B} = F(\psi)$ Helander (2014)
  - Quasi-helical (M,N integers), quasi-toroidal (N=0), quasi-poloidal (M=0)
- Quasi-omnigeneity can further improve closed contour configurations
  - $J = \oint v_{\|}\, dl = J(\psi)$
  - Constant |B| contour spacing

    Cary, Shasharina (1997)

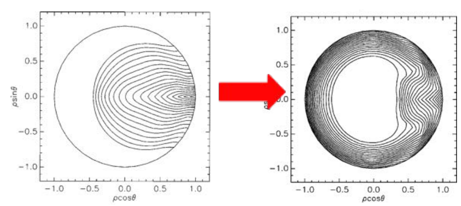

D. Spong, S. Hirshman, et al. (first use of STELLOPT, 1998)

- B_{min} and B_{max} contours
  - Min/max along field line make const. on flux surface
  - Deeply trapped: $B_{min}(\psi)$, Transitional: $B_{max}(\psi)$

Oak Ridge National Laboratory

3 methods for creating rotational transform

(L. Spitzer, 1951; C. Mercier, 1964)

Rotational transform (= 1/q) profiles

- Plasma current (3D tokamak)
- Planar axis, rotating cross-section (LHD, ATF)
- Helical magnetic axis (TJ-II, HSX, W7-X,

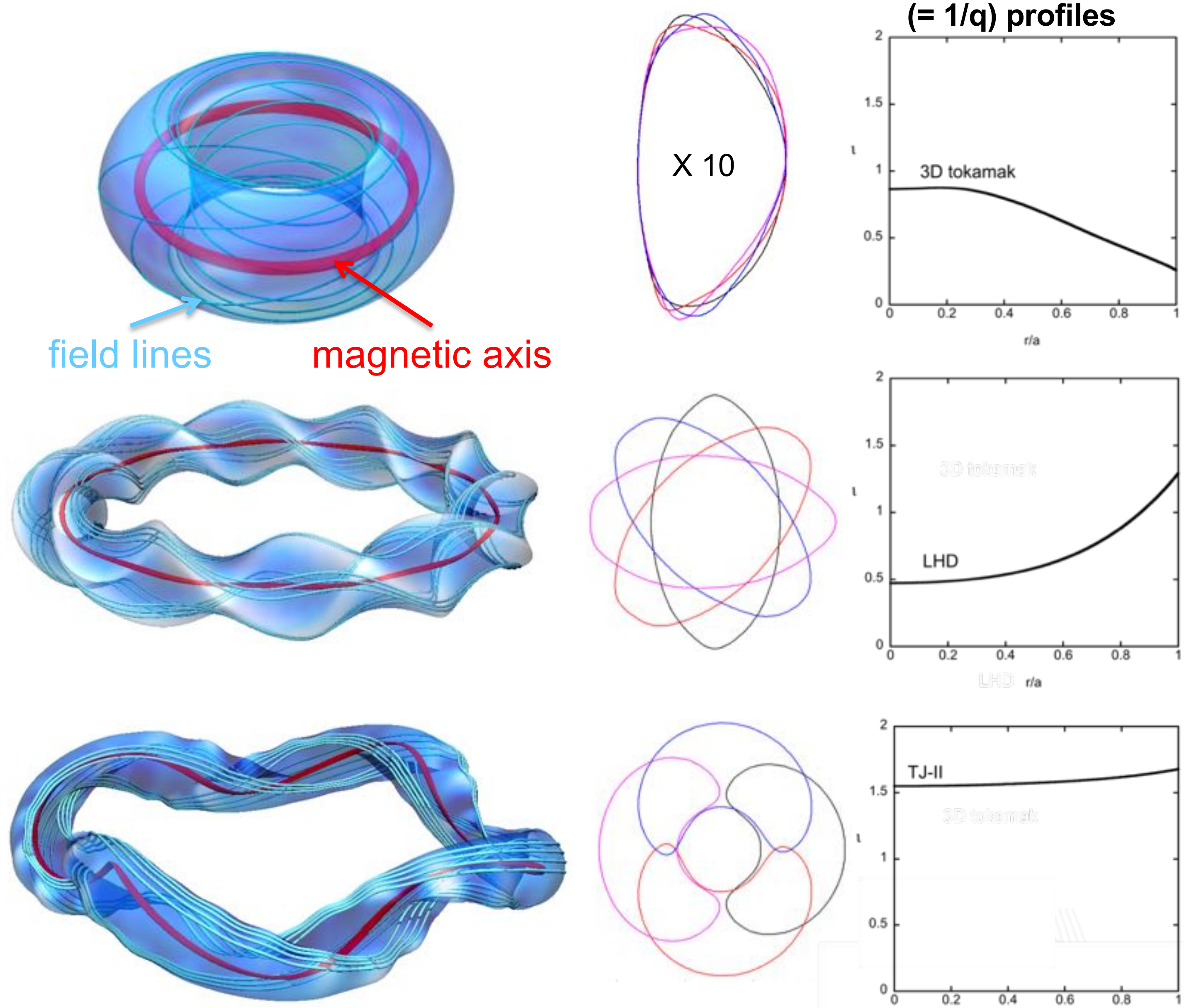

Configuration scaling: ι / N_{fp} = const., <R>/<a>/ N_{fp} = const., N_{fp} = field periods

- **Stellarator/tokamak hybrids**
  - NCSX

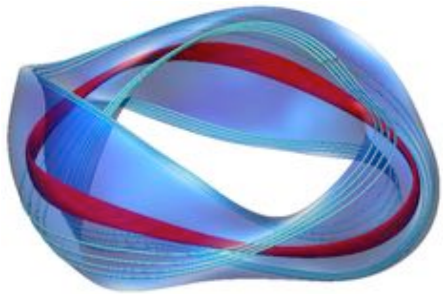
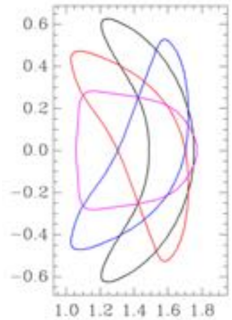
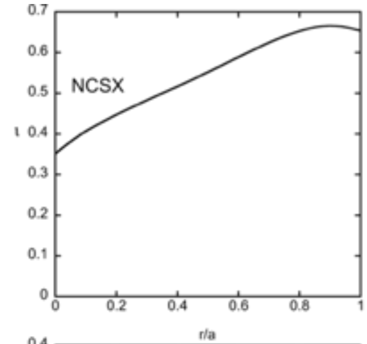

  - QPS

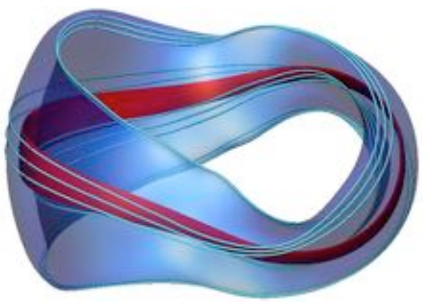
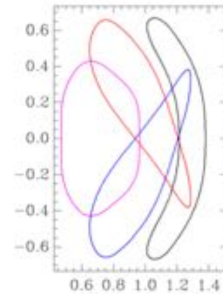
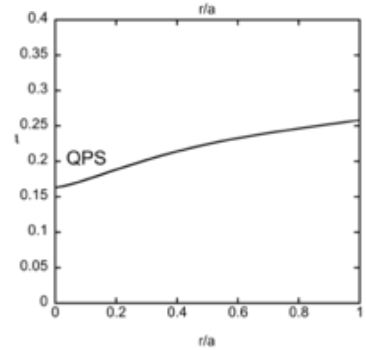

  - Tilted coils

transform amplifier

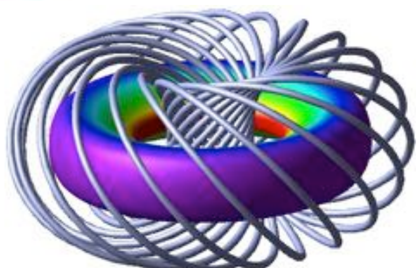

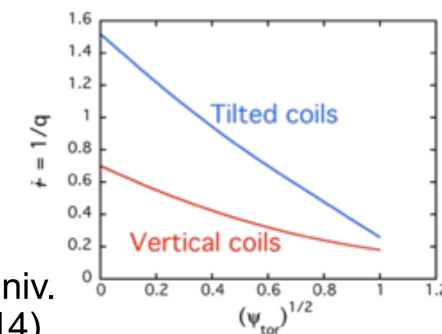

Proto-CIRCUS - Columbia Univ.
A. Clark, F. Volpe, et al. (2014)

- **Reverse field pinches**
  - single helicity states
  - sustainment, transport barriers

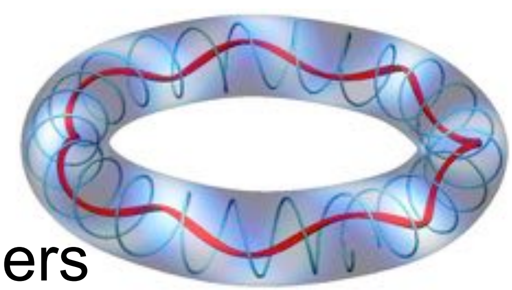
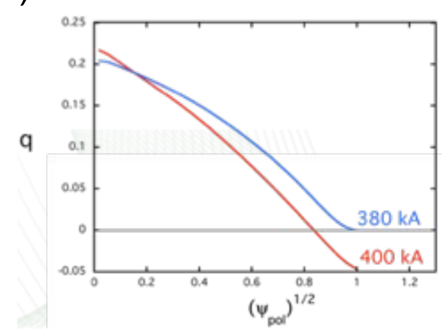

Outline

- Introduction
- **Energetic particle confinement**
  - Orbit equations and types
  - Adiabatic invariants/reduced models
  - Optimization targets
  - Configuration categorization based on closed |B| contours
- Energetic particle stability

Particle Orbits in 3D fields

- Guiding-center
  - Canonical coordinates (A. Boozer, R. White, 1981)
    - Only involves |B| and currents in straight field line coordinates

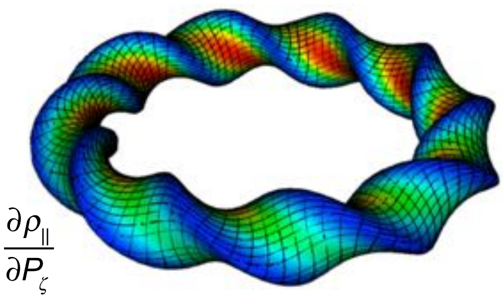

$$\frac{d\psi}{dt} = \frac{1}{D}\left(I\frac{\partial B}{\partial \zeta} - g\frac{\partial B}{\partial \theta} \right)\left(\mu + \frac{mv_{\parallel}^2}{B} \right); \qquad \frac{d\rho_{\parallel}}{dt} = \frac{\iota - \rho_{\parallel} g'}{D}\dot{P}_{\theta} + \frac{\rho_{\parallel} I'}{D}\dot{P}_{\zeta}$$

$$\frac{d\theta}{dt} = \left[\left(\mu + \frac{mv_{\parallel}^2}{B} \right)\frac{\partial B}{\partial \psi} + e\frac{\partial \Phi}{\partial \psi} \right]\frac{\partial \psi}{\partial P_{\theta}} + eBv_{\parallel}\frac{\partial \rho_{\parallel}}{\partial P_{\theta}}; \qquad \frac{d\zeta}{dt} = \left[\left(\mu + \frac{mv_{\parallel}^2}{B} \right)\frac{\partial B}{\partial \psi} + e\frac{\partial \Phi}{\partial \psi} \right]\frac{\partial \psi}{\partial P_{\zeta}} + eBv_{\parallel}\frac{\partial \rho_{\parallel}}{\partial P_{\zeta}}$$

  - Non-canonical coordinates (Littlejohn, Cary 1979-83)
    - Lie-transform perturbation methods, variational action integral
    - Coordinate-free

$$\frac{d\vec{R}}{dt} = \frac{1}{B_{\parallel}^*}\left(\mathrm{v}_{\parallel}\vec{B}^* + \vec{E}^* \times \hat{b} + \frac{\mu \hat{b} \times \vec{\nabla} B}{Ze} \right); \quad \frac{d\mathrm{v}_{\parallel}}{dt} = Ze\left(\vec{E}^* + \vec{R} \times \vec{B}^* \right)\mu \vec{\nabla} B$$

$$\vec{B}^* = \vec{B} + \frac{m\mathrm{v}_{\parallel}}{Ze}\vec{\nabla} \times \hat{b}; \quad \vec{E}^* = \vec{E} - \frac{m\mathrm{v}_{\parallel}}{Ze}\frac{\partial \hat{b}}{\partial t}$$

  - Adiabatic invariants: $\mu = m\mathrm{v}_{\perp}^2/2B$, $J=\oint m\mathrm{v}_{\parallel}$, $\vec{\mathrm{v}}_d=\vec{\nabla} J \times \hat{b}/Ze$

- Lorentz equation: $\dfrac{d\vec{\mathrm{v}}}{dt} = \dfrac{Ze}{m}\left(\vec{E} + \vec{\mathrm{v}} \times \vec{\mathrm{B}} \right)$ G.C.

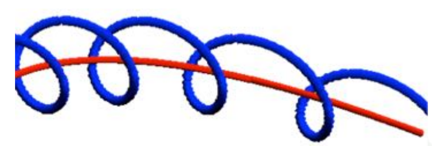

Issues for simulations: energy conservation, Liouville's theorem (conservation of phase space volume carried with particle), intersections of fast ion with walls, PFCs

$$\frac{1}{\sqrt{g}}\frac{\partial}{\partial z^i}\left(\sqrt{g}\frac{\partial z^i}{\partial \tau} \right) = 0$$

Particle trajectories in 3D configurations: many new classes of orbits

Stellarator (E_r added for confinement of trapped and transitional orbits)

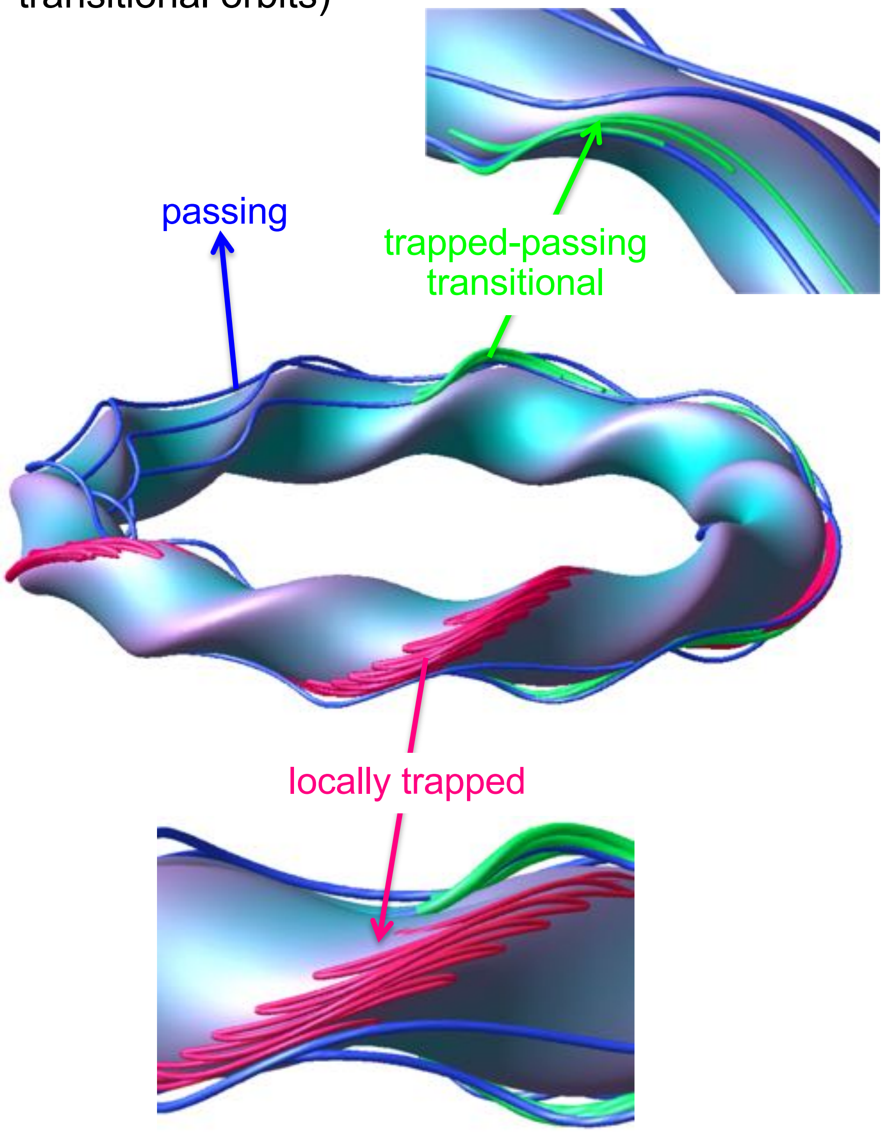

Tokamak with ripple and TBM

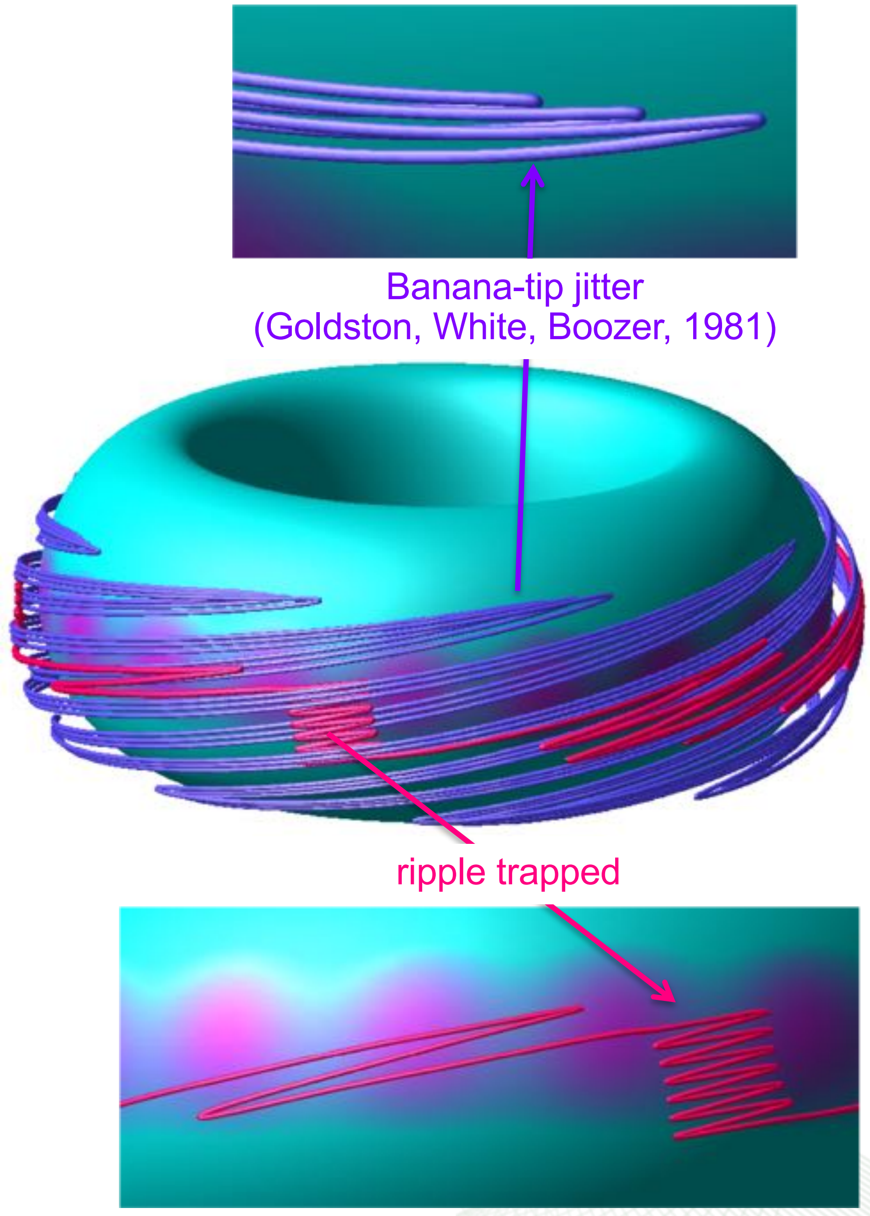

J optimization – simplest to apply to ≥ 5 field period QO systems, but should be extendable to other configurations (QH, QA)

$$J = \oint \frac{dl}{v_{||}}$$

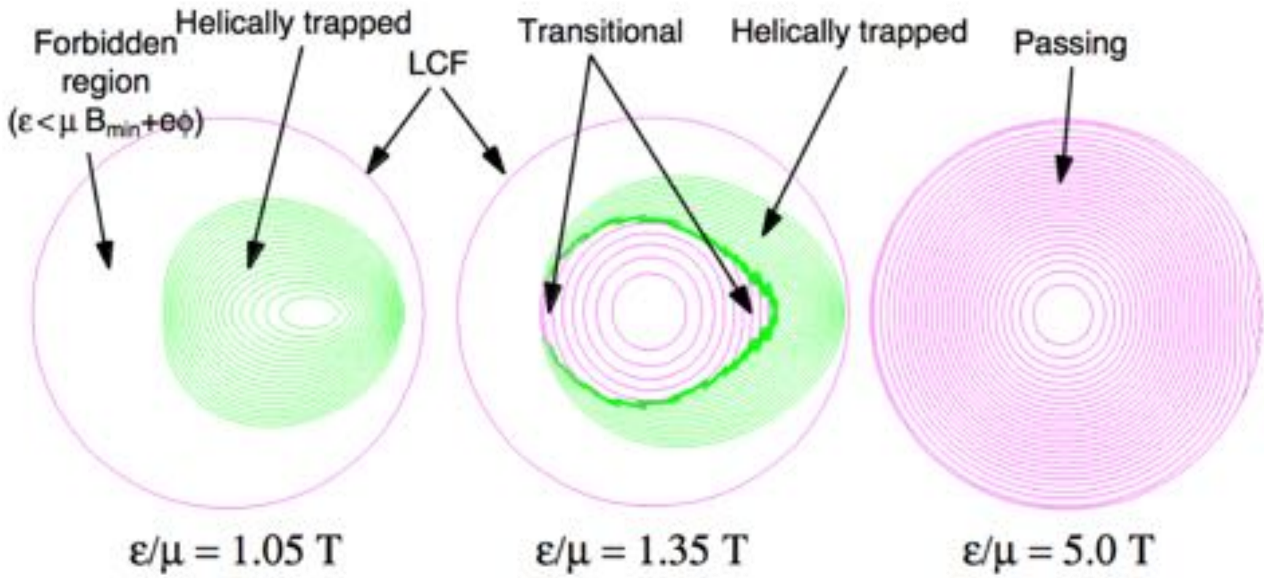

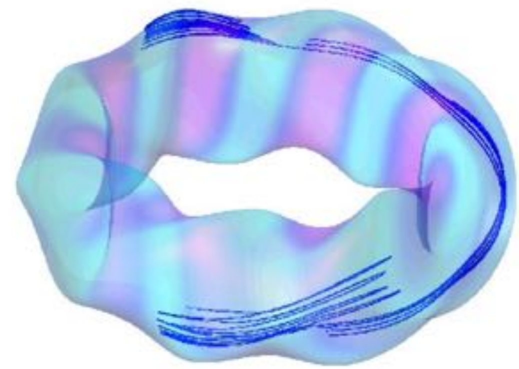

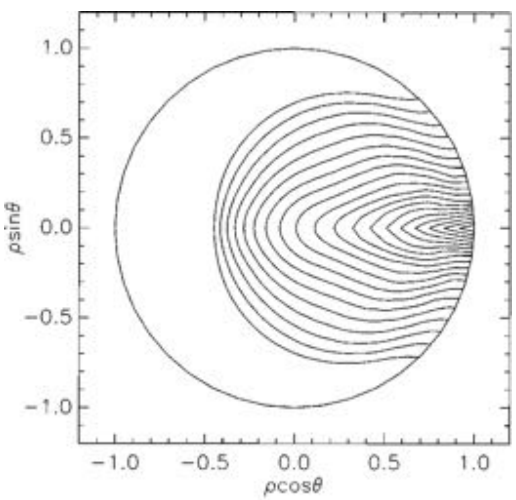

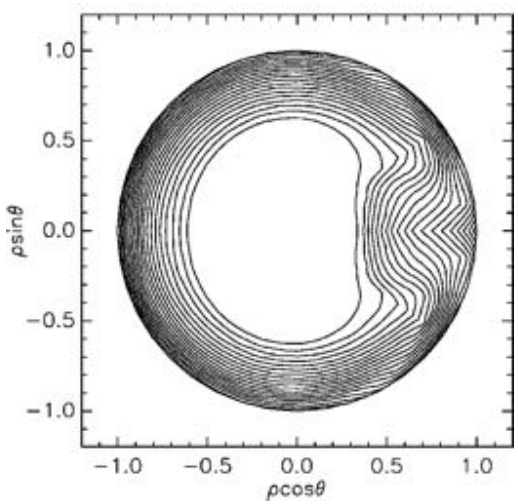

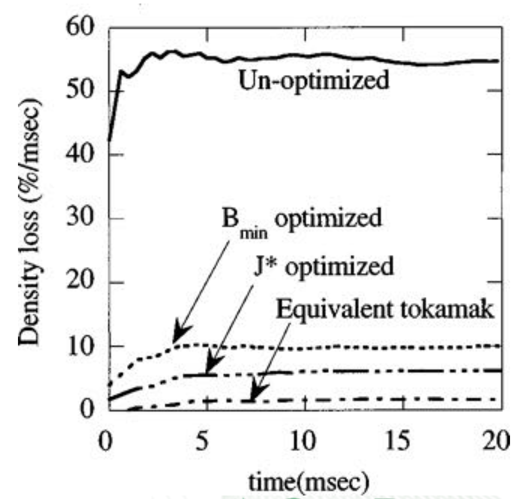

D. Spong, et al., POP (1998)

J optimization (contd.)

Large aspect ratio QO configuration
[Mikhailov, Shafranov, Nührenberg, et al, Nuclear Fusion 2002]

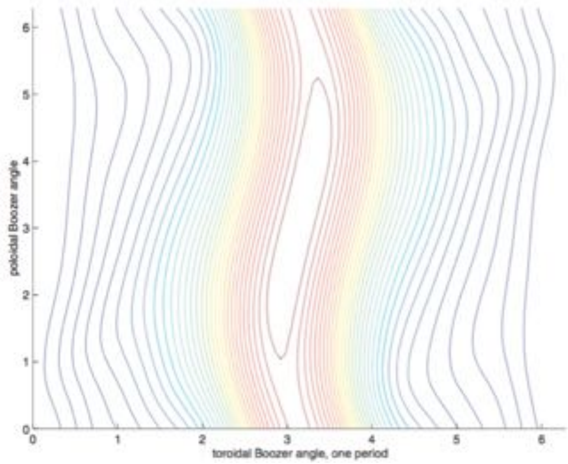

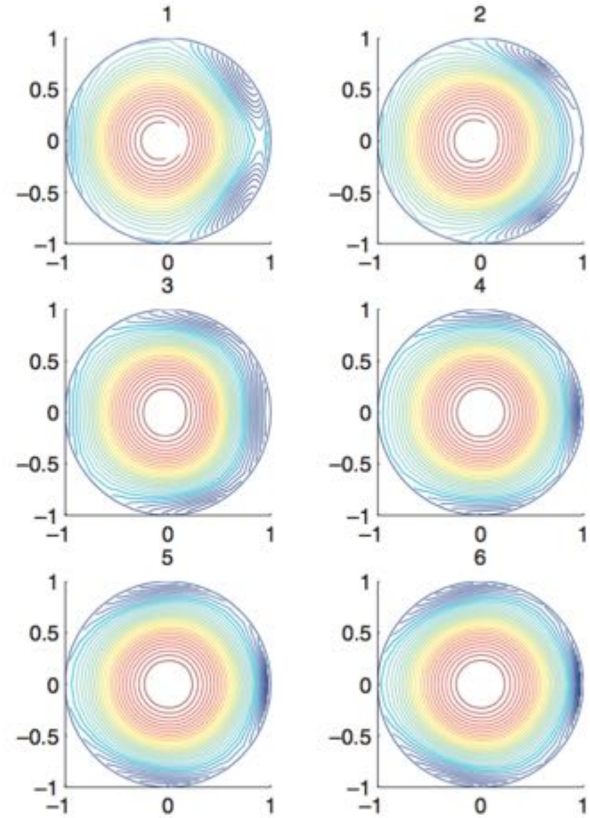

Finite β effects on J contour centering [A. Ware, S. Hirshman, et al., PRL 2002]

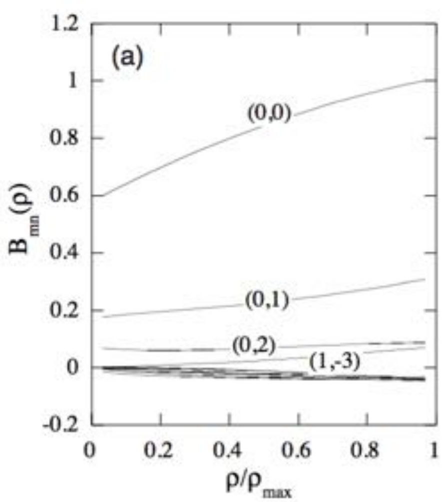

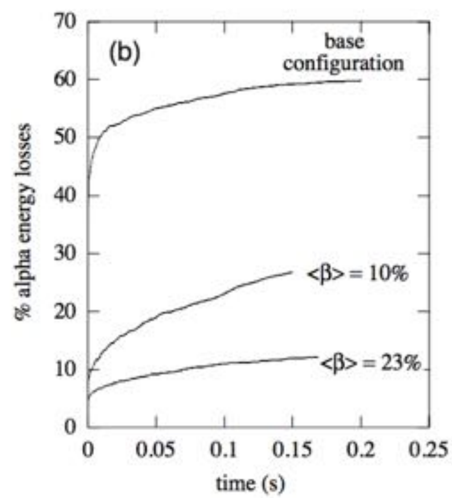

Also, significant improvements in J seen for W7-X at $\beta \sim 5\%$

OAK RIDGE National Laboratory

EP confinement improvements

- Bounce/velocity-averaged radial drift parameter (analogous to NEO ε_{eff} for low ν transport)

$$\Gamma_w = \frac{\pi R_0^2}{\sqrt{2}} \lim_{L_s\to\infty}\left(\int_0^{L_s}\frac{ds}{B}\right)^{-1}\frac{1}{\langle|\nabla\psi|\rangle^2} \times \int_{B_{\min}^{\mathrm{abs}}/B_0}^{B_{\max}^{\mathrm{abs}}/B_0} db' \sum_{j=1}^{j_{\max}}\left(\frac{\partial g_j}{\partial b'}\right)^2\left(\frac{\partial \hat{I}_j}{\partial b'}\right)^{-1}$$

For $B \approx B_0[1+\epsilon_h\cos(m\theta - n\varphi)]$

$$\Gamma_w^{(\mathrm{conv})} = \sqrt{\epsilon_h}$$

V. Nemov, S. Kasilov, W. Kernbichler, G. Leithold, POP 2005

- Monte Carlo
  - Mynick, Boozer, Ku (POP, 2006) find NCSX fast ion confinement improved by adding mirror term: local well near magnetic peak vs. in magnetic slope region
  - Reactor size NCSX α losses reduced from 27% to < 10%
  - Particle noise may favor genetic or differential evolution optimization methods

OAK RIDGE National Laboratory

Outline

- Introduction
- Energetic particle confinement
- **Energetic particle stability**
  - EP turbulence impacts confinement
  - Categories of EP instability
  - Alfvén instability basics: gap structure, eigenmodes
  - Gyrokinetic models – full/reduced
  - Gyrofluid models – application to LHD and TJ-II
  - Methods for controlling EP instabilities

Fast ion instabilities and confinement

- Tokamaks show 40-60% of fast ion energy can be lost when EP instabilities are present [DIII-D, W. Heidbrink, Nuclear Fusion **48** (2008)]

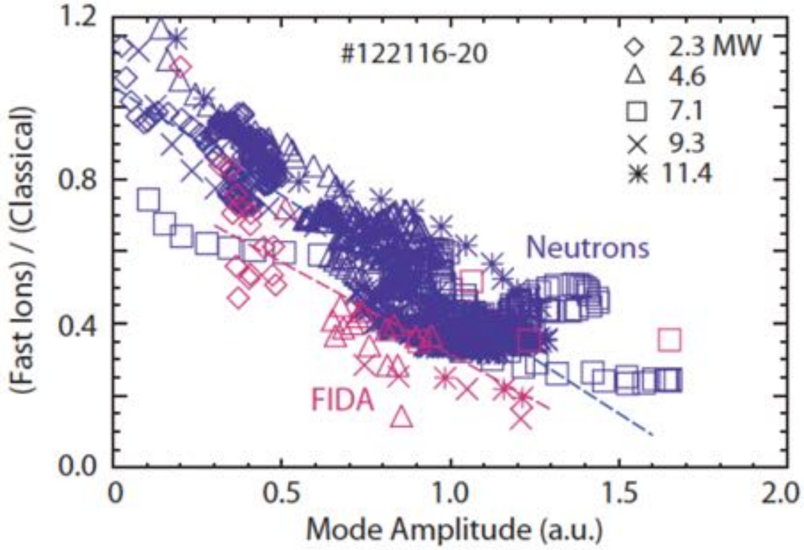

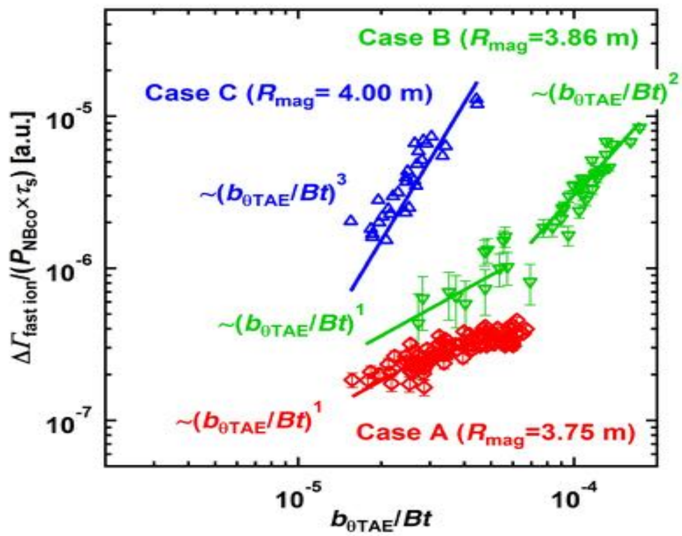

Loss scaling in LHD – K. Ogawa

- Stellarator options for mitigation
  - High density operation
  - ECH suppression (as in tokamaks, M. Van Zeeland, et al.)
  - ECCD => modify iota (Heliotron-J)
  - Direct optimization of Alfvén gap structures

OAK RIDGE National Laboratory

Stellarator reactors at high density sample a different EP regime than tokamaks

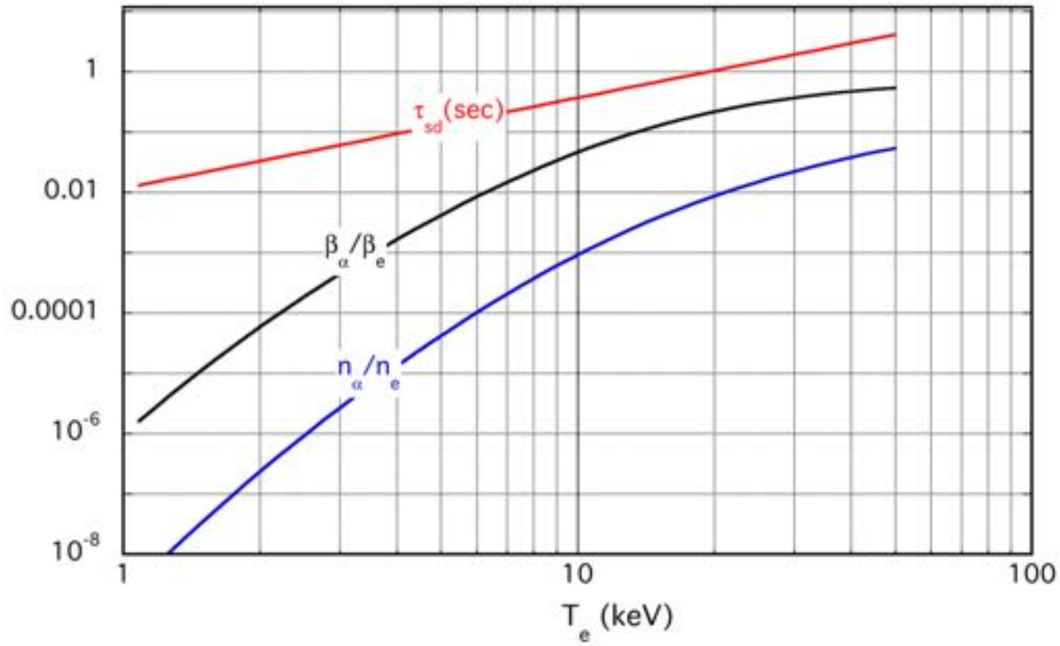

- At steady-state $\frac{n_\alpha}{\tau_{s\alpha}} = \frac{n_e^2}{4}\langle\sigma_f \mathrm{v}\rangle$ D. Sigmar, et al. Phys. Scripta 1987
- Since $\tau_{s\alpha} \propto {T_e^{3/2}}/{n_e}$, $\frac{n_\alpha}{n_e}$ depends only on T_e *(for $T_e = T_i$)*

Stellarator reactors at high density sample a different EP regime than tokamaks

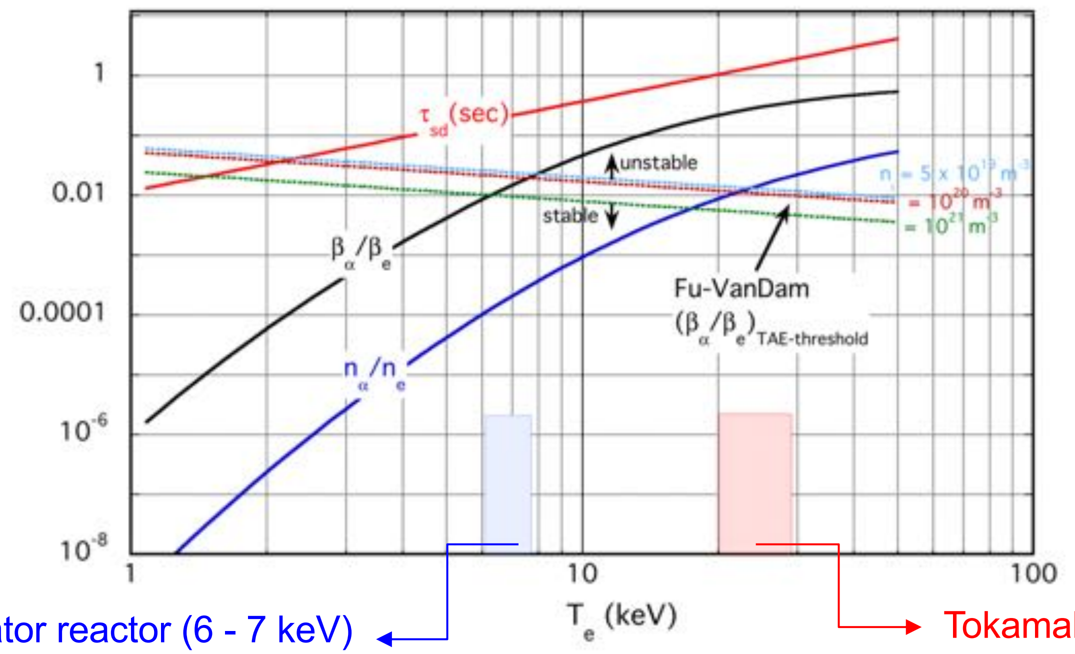

High density stellarator reactor (6 - 7 keV)

Tokamak reactor (20 – 30 keV)

- AE stability limits also scale with T_e, (with a weak density dependence), e.g., Fu-Van Dam (1989)

$$\beta_\alpha\left(\frac{\omega_{*\alpha}}{\omega}-\frac{1}{2}\right)F > \beta_e\frac{v_A}{v_e} \text{ where } F = x(1+2x^2+2x^4)e^{-x^2} \quad x = \frac{v_A}{v_\alpha}$$

- N. Ohyabu, et al., PRL 2006 consider low temperature, high density reactor with $T_{e,i}$ = 6 to 7 keV
  - But thermal stability feedback loop: rising T => more alpha heating

Stellarator reactors at high density sample a different EP regime than tokamaks

High density/low T reactor may be able to stay on stable side of AE's

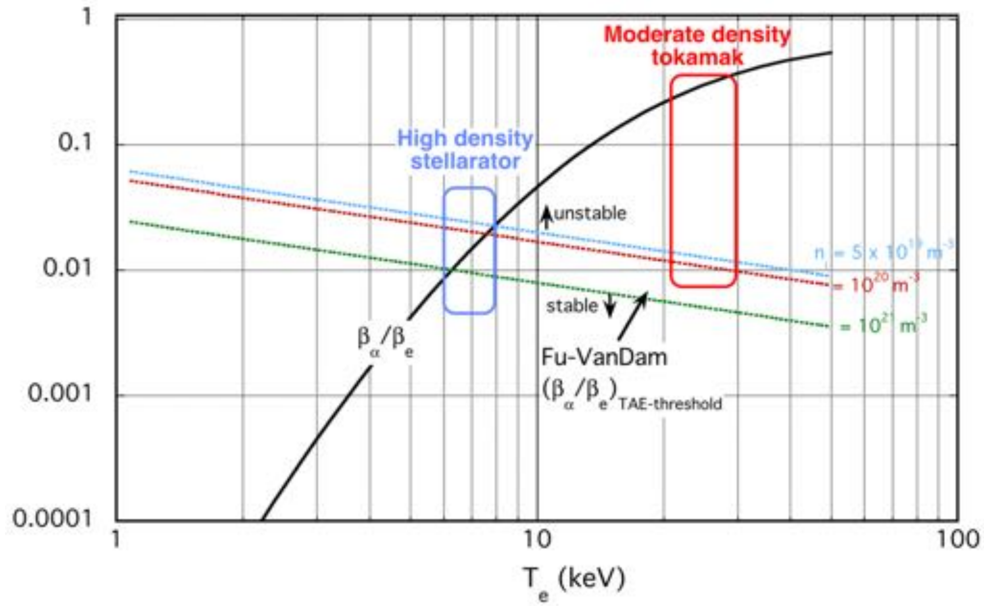

High density increases energy scattering range/minimizes lossy pitch angle scattering range

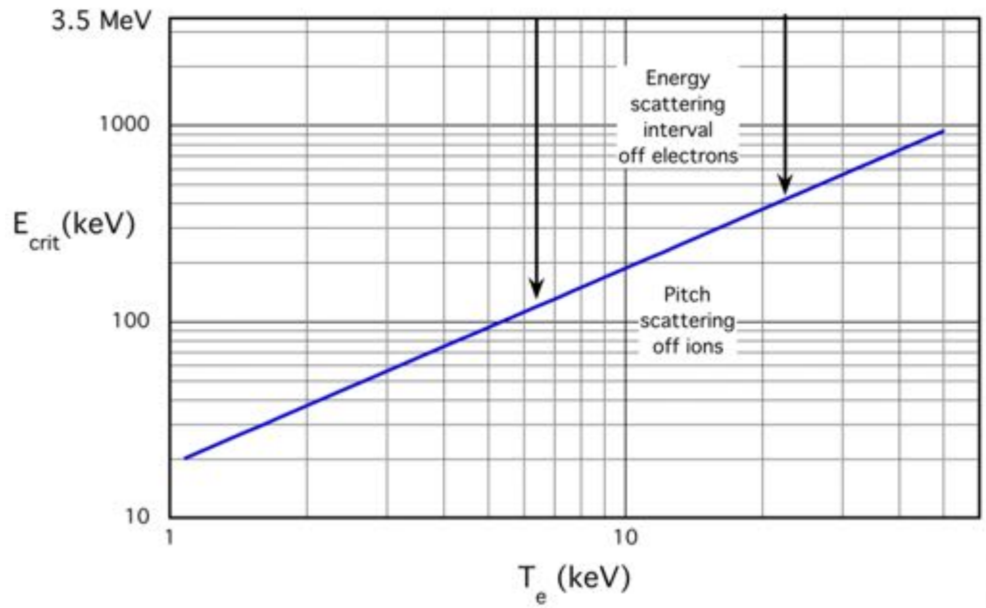

Oak Ridge National Laboratory

Categories of EP-driven instability

- **Thermal plasma-driven MHD instabilities that are augmented or suppressed by energetic particles**
  - EIC mode, fishbones, sawteeth, infernal modes
- **Stable MHD waves that are destabilized by EP**
  - ★AE modes (★ = T, G, H, M, C, RS, B, BA, …)
  - Can be classified as gap (mode coupled) or extremal modes
- **Some possible good effects**
  - Channeling: direct transfer of EP energy to core ions
    - Beta-induced Alfvén and acoustic Alfvén modes (BAE, BAAE)
  - Alpha ash removal
- But, since highest energy EP component can be rapidly transported, deleterious for PFC's and power balance

A growing collection of models/codes are available for AE's in 3D systems

- Alfvén continua and gaps
  - CAS3D, **STELLGAP***
- Stable Alfvén modes
  - CAS3D, **AE3D***
- Perturbative stability models
  - CAS3D-K, AE3D-K, CKA-EUTERPE
- AE resonance mapping
- Hybrid fluid particle models
  - MEGA, M3D-K
- Gyrofluid: FAR3D
- Gyrokinetic: GTC, GENE, GS2, EUTERPE

*Available on GITHUB

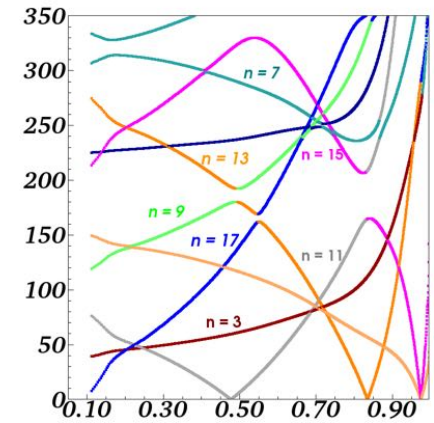

TJ-II continuum gaps

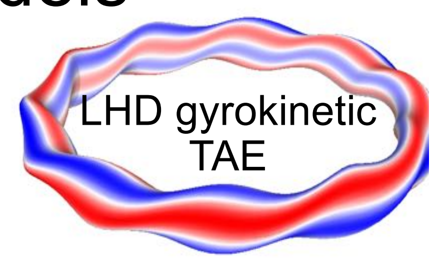

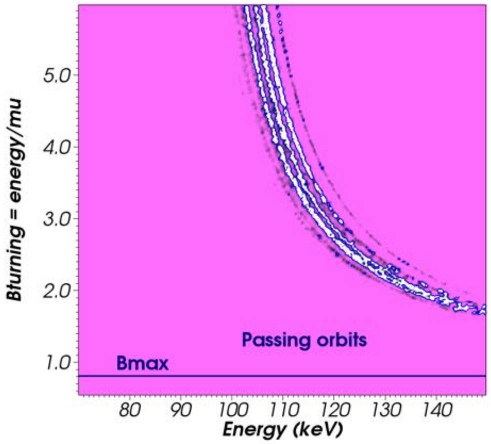

LHD particle-AE resonance map

Oak Ridge National Laboratory

Open/closed Alfvén gaps: show which modes are viable for destabilization

Effective inertia along magnetic field line ~ $n_{ion} m_{ion} / B^2$

Bending energy ~ $k_{\parallel}^2 = \frac{1}{qR}(nq - m)^2 \quad n, m = \text{integers}$

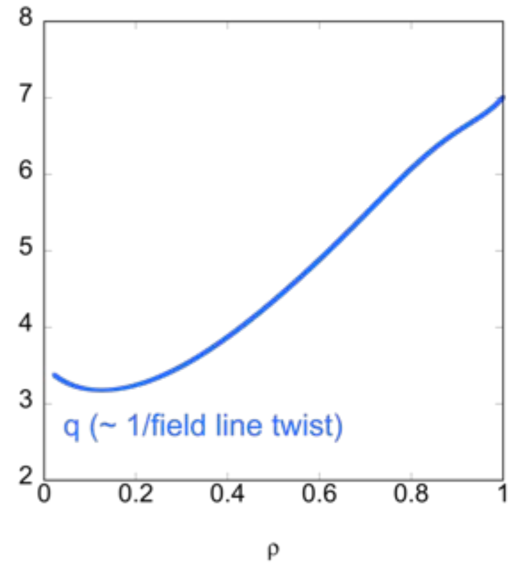

Cylindrical n = 3 Alfvén continua: $\omega^2 = k_{\parallel}^2 v_A^2$

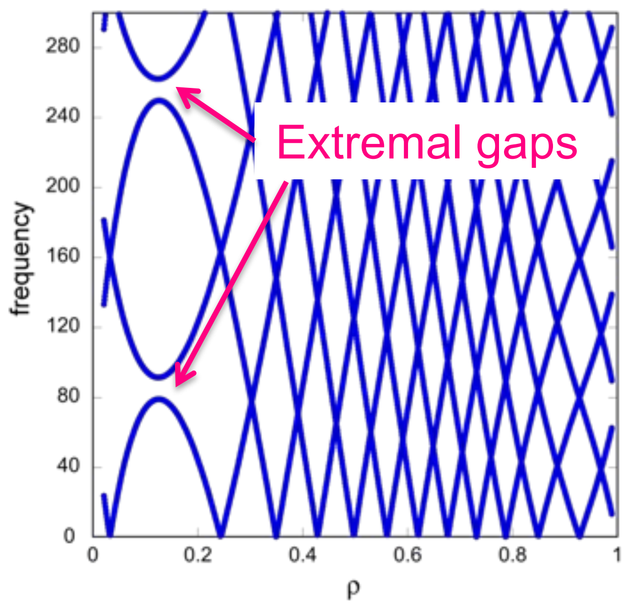

$$\frac{\partial k_{\parallel} v_A}{\partial r} = 0;\ k_{\parallel,m} \neq -k_{\parallel,m+1}$$

Toroidal n = 3 Alfvén continua

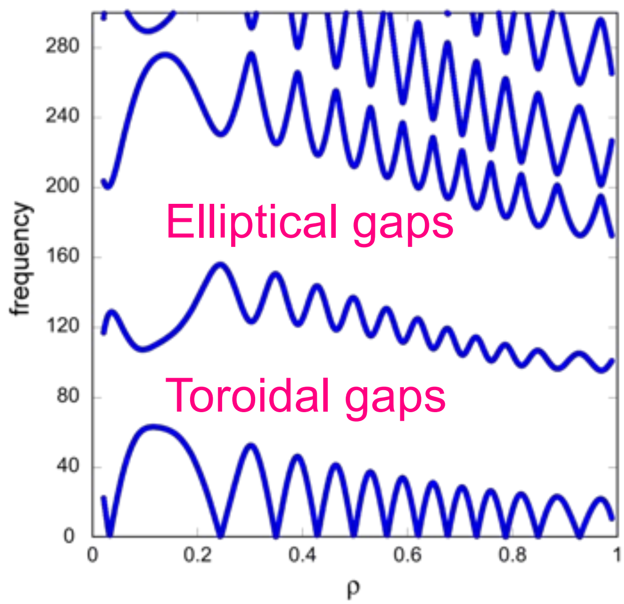

$$k_{\parallel,m} = -k_{\parallel,m\pm1}$$

Toroidal n = 3 Alfvén-acoustic continua

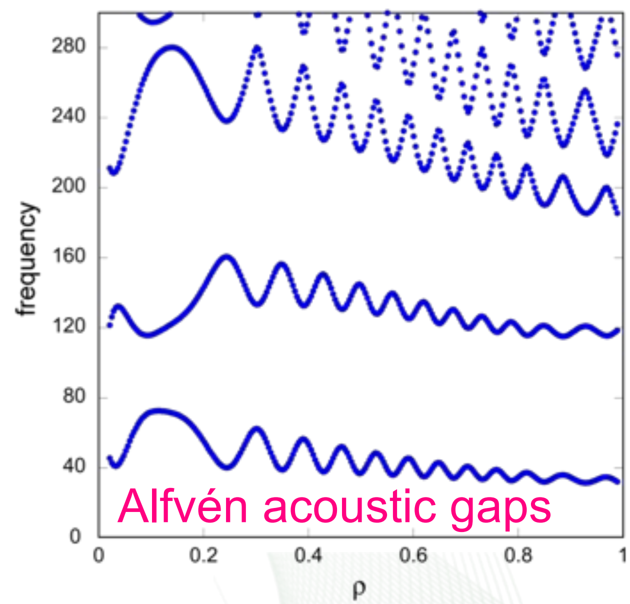

$$k_{\parallel,m} v_A = -k_{\parallel,m'} C_S$$

Toroidal mode number (n) is not a good quantum number for 3D configurations

- Field period symmetry: N_{fp} replicated elements
- Toroidal coupling => mode families, rather than single toroidal modes:

  $n' \pm n = kN_{fp}$, k = 0, 1, 2, …

- Finite number of families: $1 + N_{fp}/2$ for even N_{fp} and $(N_{fp}-1)/2 + 1$ for odd N_{fp}
- Computational difficulty
  - High N_{fp} easiest
  - Low N_{fp} hardest

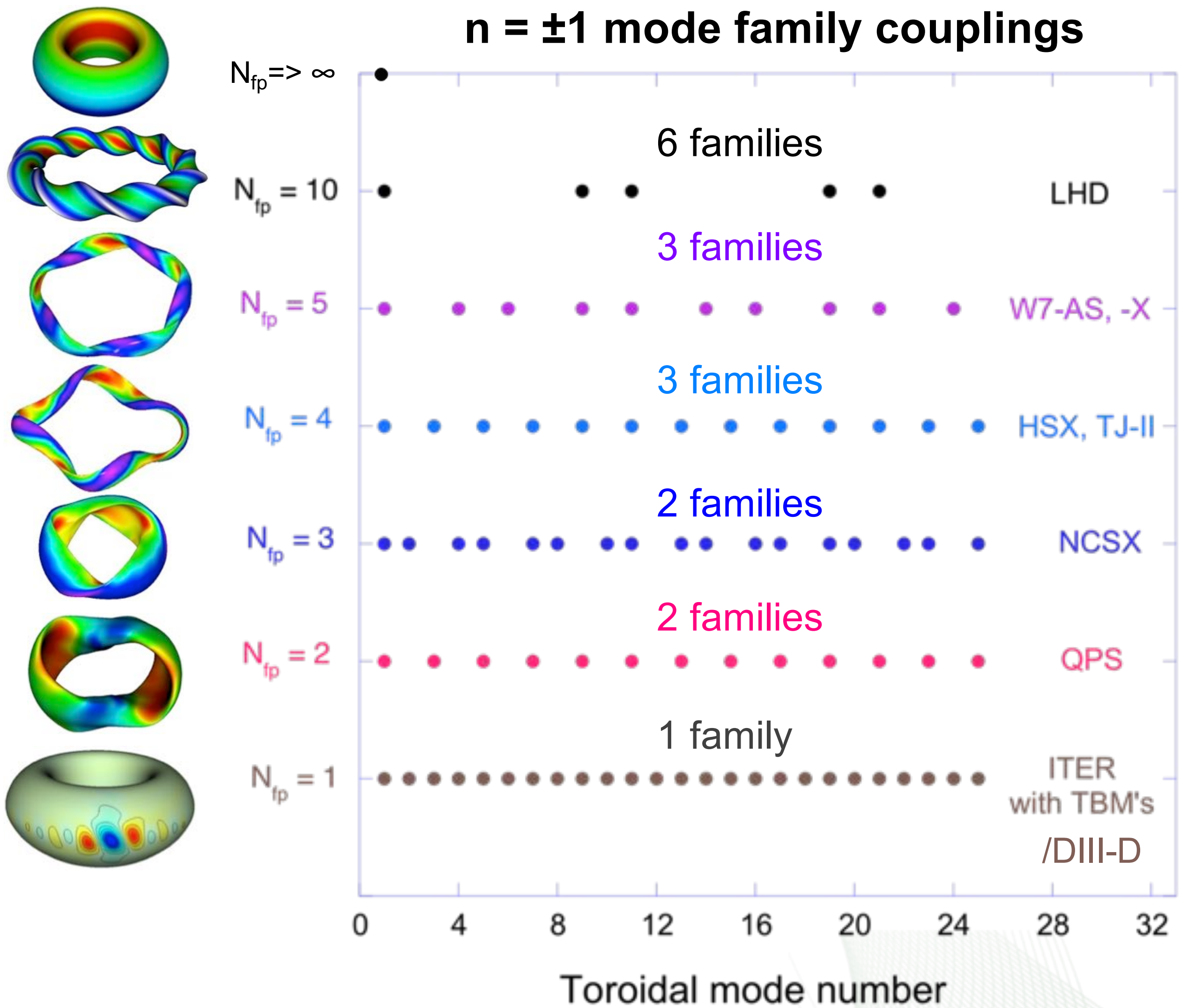

Stellarators include both tokamak-like Alfvén gaps as well as ones unique to 3D (helical and mirror Alfvén gaps)

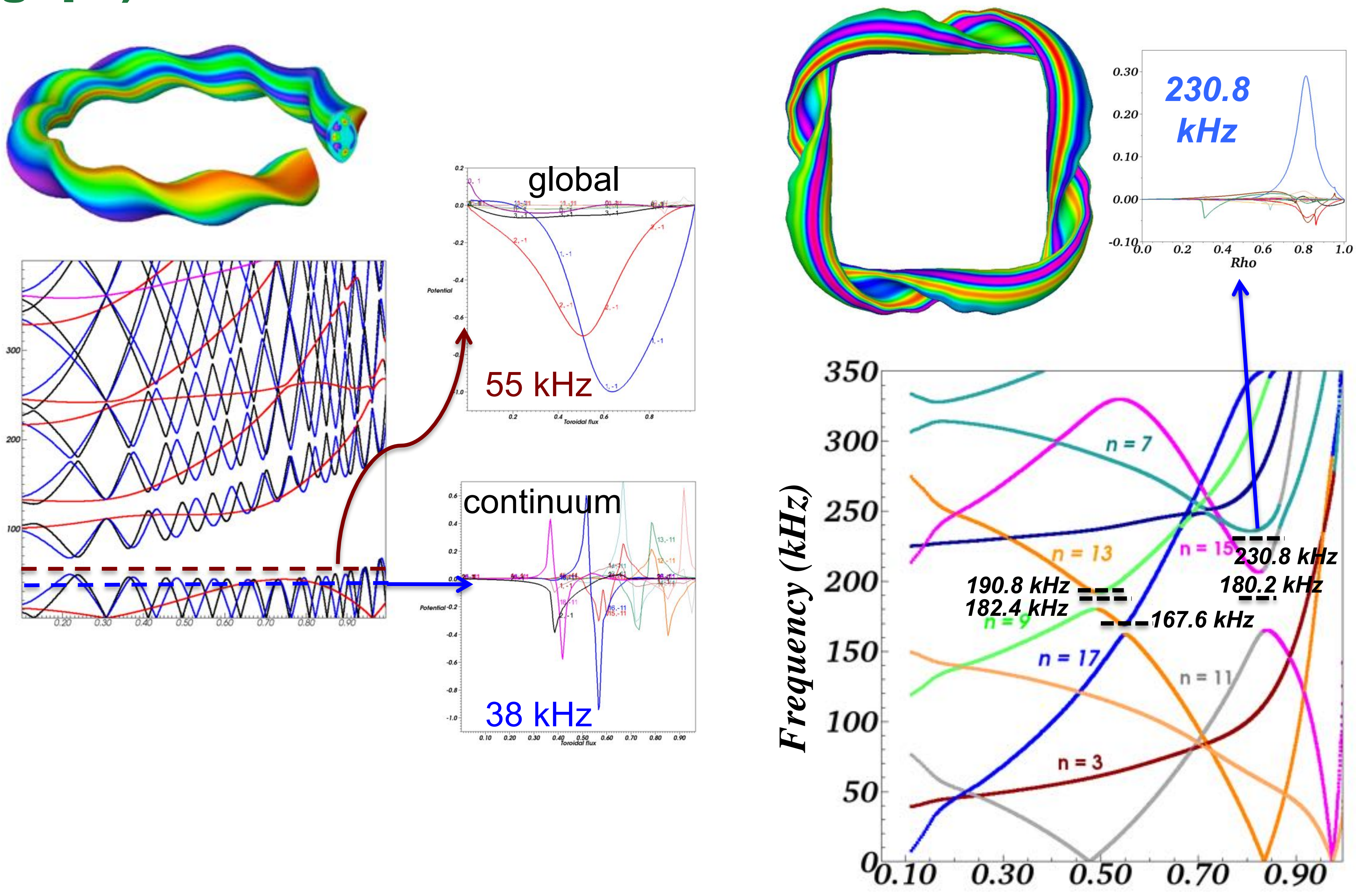

Gyrokinetic models for 3D configurations

- **Reduced vs. complete models**
  - Perturbative linear wave-particle energy transfer model
  - Global δf PIC or continuum models
    - GEM: flux tube approach generalized to flux surface – each field line different in 3D
    - Global: GTC, EUTERPE
- **Kinetic ions, fast ions: full GC orbits followed**
  - charges, currents allocated over local gyro radius template for field solve
  - Maxwellian, slowing-down distribution options
- **Several options for electron and field models**
  - Adiabatic, Fluid/hybrid, Fully kinetic
  - Electrostatic (ITG), electromagnetic (Alfvén instability)

OAK RIDGE
National Laboratory

Linear gyrokinetic wave-particle energy transfer method:

$$\gamma \propto \frac{\int \overrightarrow{\delta J}_{particles} \cdot \vec{E}}{Wave\ energy}$$

D. Spong, et al., Contr. to Plasma Physics **50** (2010) 708.

A. Mischenko, et al., NF (2014).

- Used in AE3D-K, EUTERPE, and VENUS codes

n = 1, -9 continuum structure

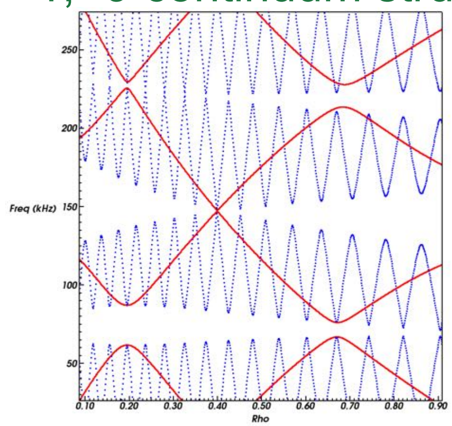

LHD TAE mode

B = 3.1T, $n_{fast}(0) = 1.2 \times 10^{18}\ m^{-3}$

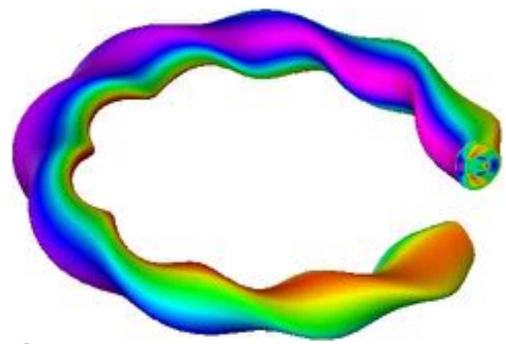

Stable AE mode structure

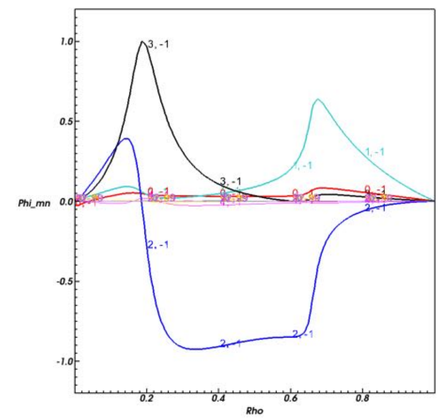

Time-average growth rates

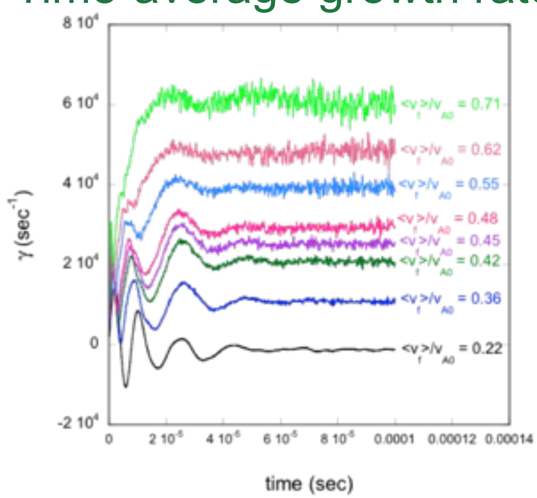

Distribution function sensitivity

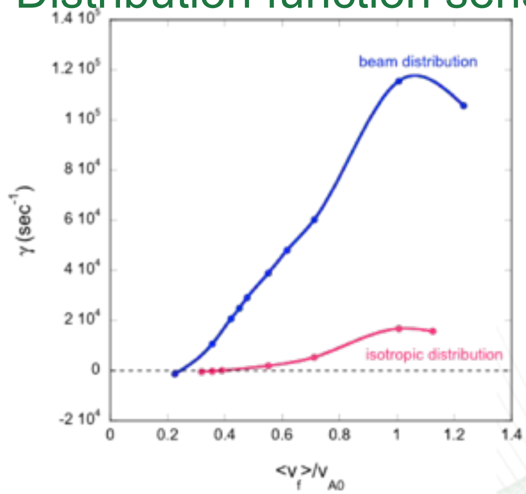

Gyrokinetic modeling of 3D systems

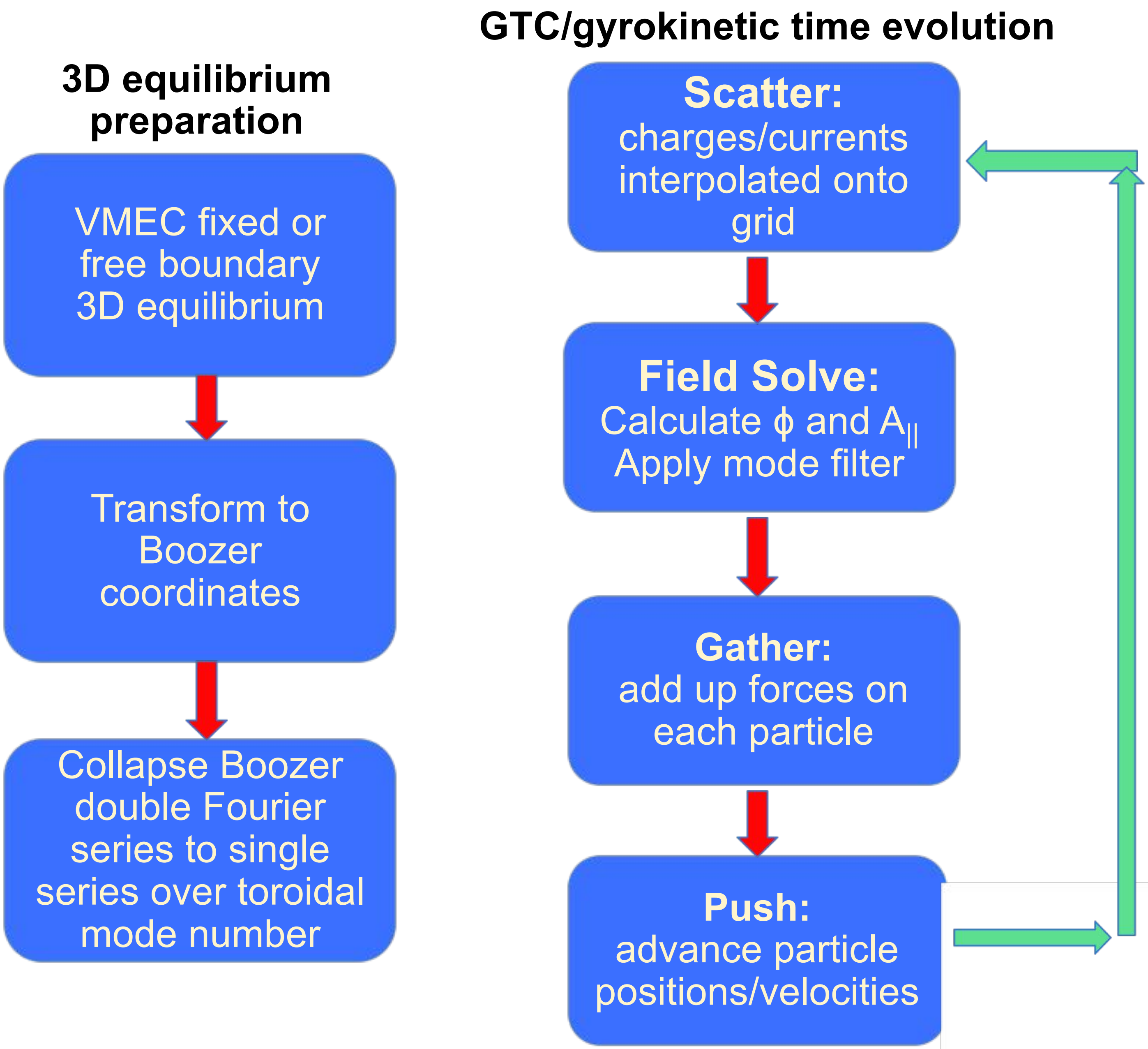

GTC modeling of AE instabilities in LHD

D. Spong, I. Holod, Y. Todo, M. Osakabe, Nuclear Fusion (2017)

- Equilibrium and profiles

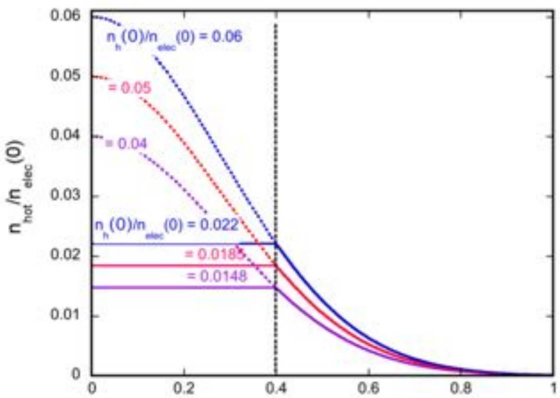

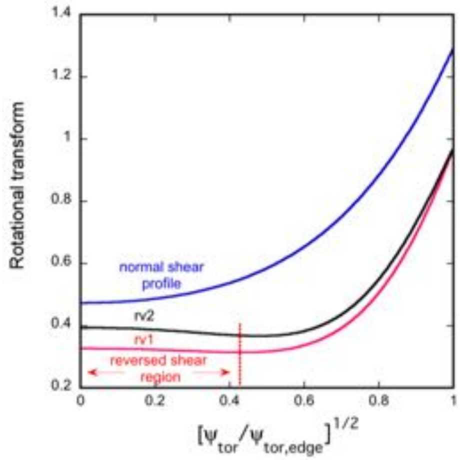

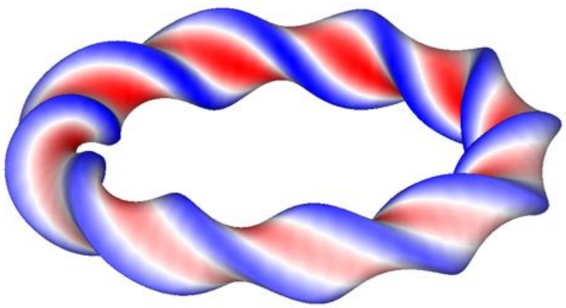

- Typical Alfvén instablility evolution

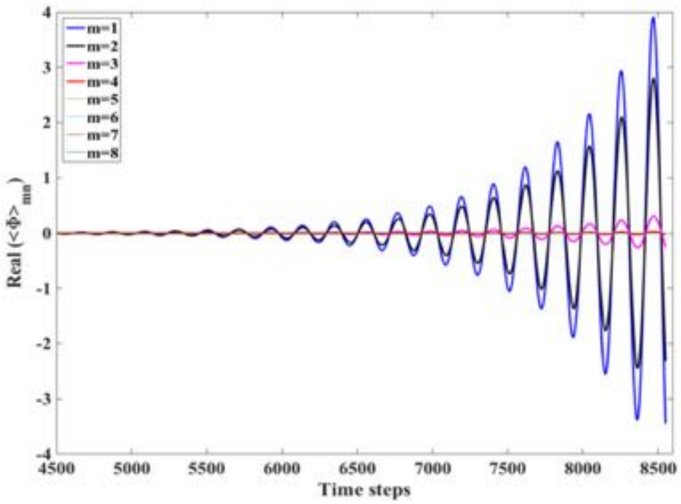

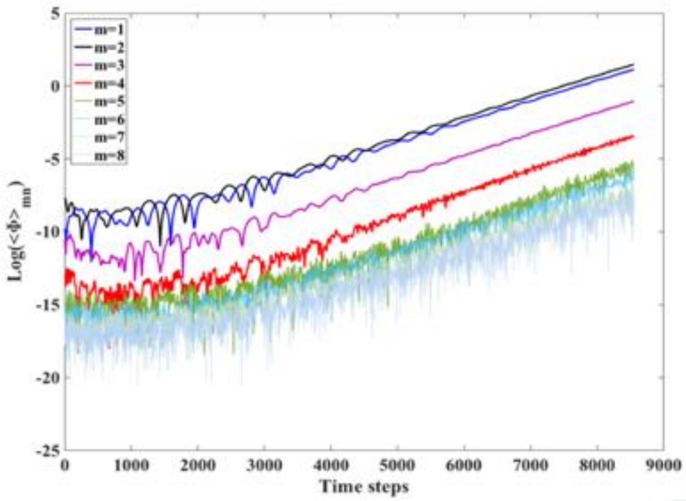

OAK RIDGE National Laboratory

GTC finds linear EP-driven modes with frequencies aligned with the primary TAE continuum gaps

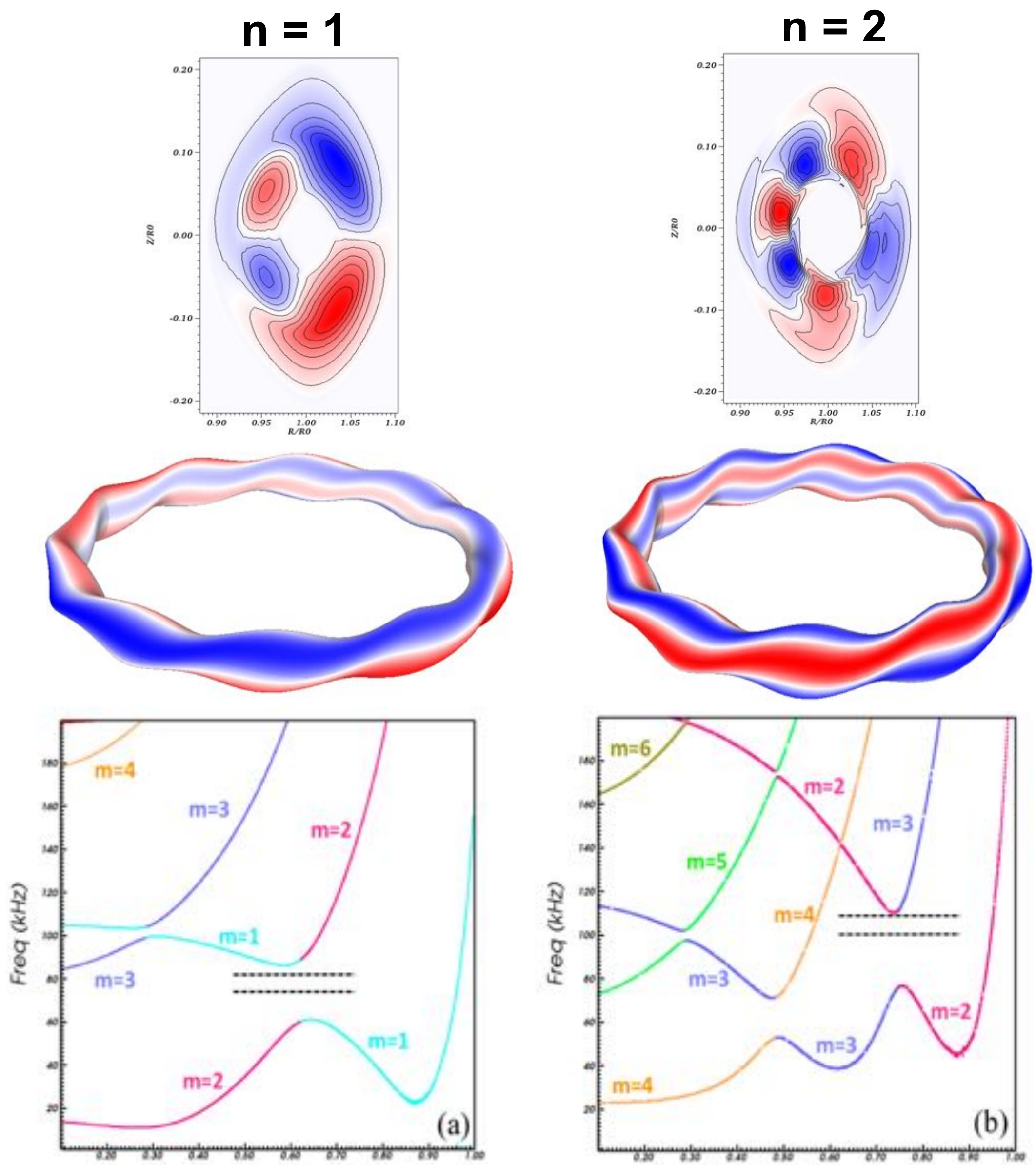

OAK RIDGE
National Laboratory

The GTC model has been applied linearly and nonlinearly for several different 3D configurations (2015 ISHW)

LHD n = 3 BAE instability

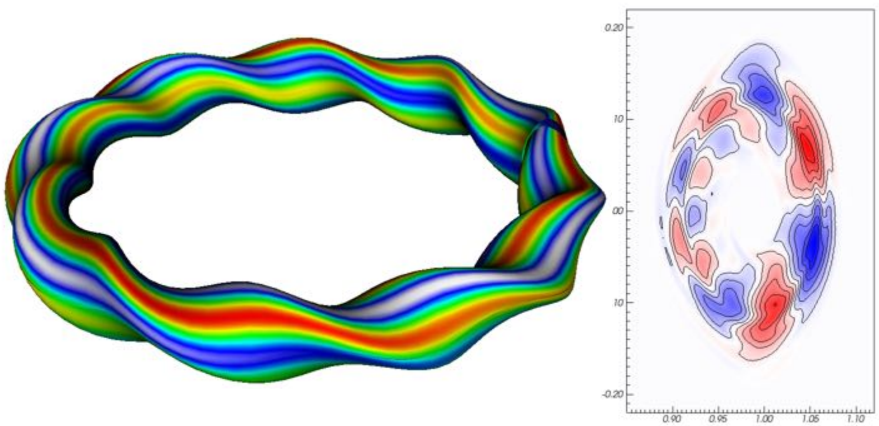

W7-X n = 6 TAE instability

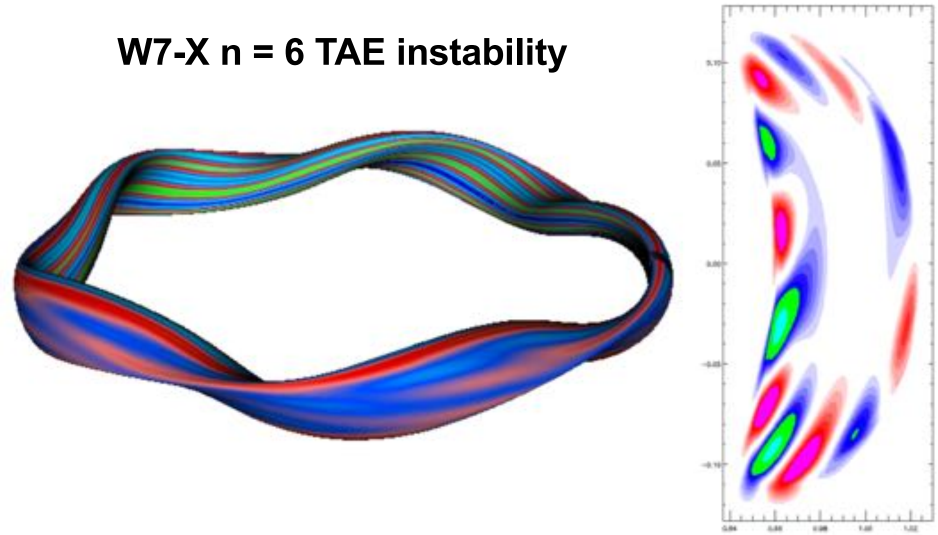

2015 JIFT exchange collaboration with Y. Todo – comparison with MEGA

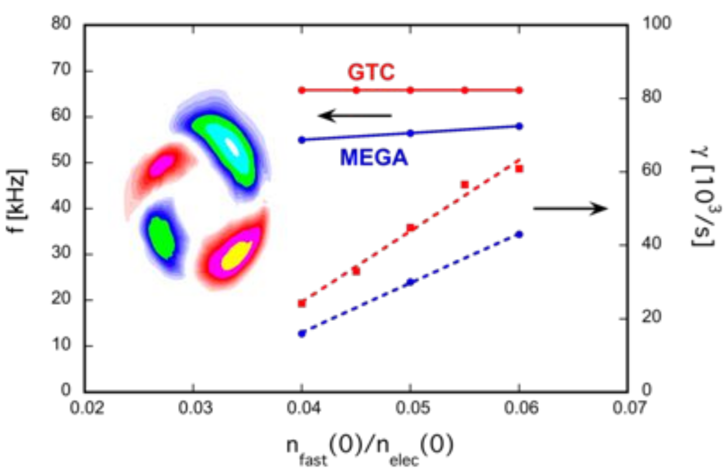

Nonlinear n = 1 evolution in LHD

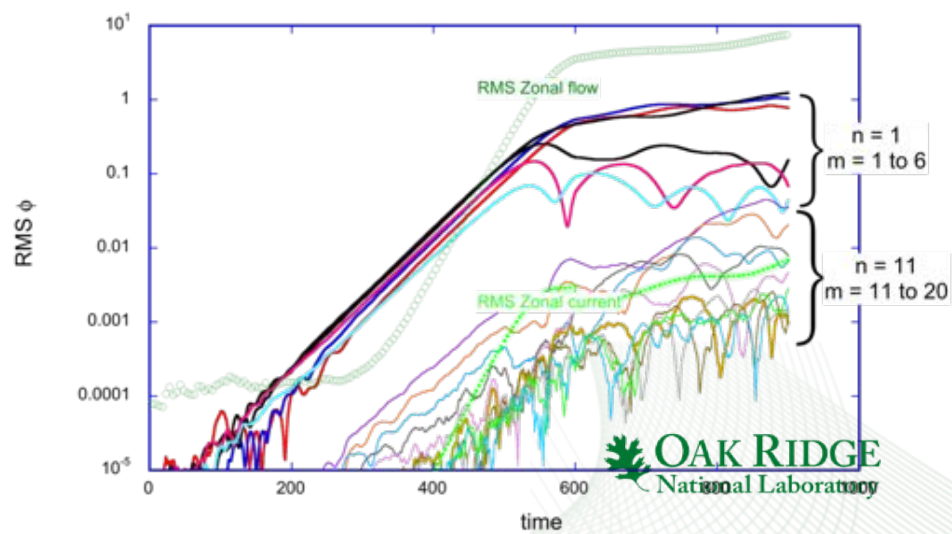

Efficient reduced dimensionality method: gyrofluid

- TAEFL (tokamak only) => FAR3D (tokamak&stellarator)
- MHD + gyrokinetic moments/Hammett-Perkins closure
- ~ 1000 times faster than gyrokinetic models
  - Good for parameter scans, Potential for optimization target
- Solution methods
  - Initial value – fastest growing instability
  - Eigenvalue hunting => can find multiple/sub-dominant modes

Tokamak:
D. Spong, B. A. Carreras, C. L. Hedrick, Phys. Fluids **B 4** (1992)
D. Spong, Nuclear Fusion **53** (2013)

LHD: J. Varela, D. Spong, et al., Nuclear Fusion (2017)

TJ-II: J. Varela, D. Spong, et al., Nuclear Fusion (2018)

2018 RSAE Benchmark study

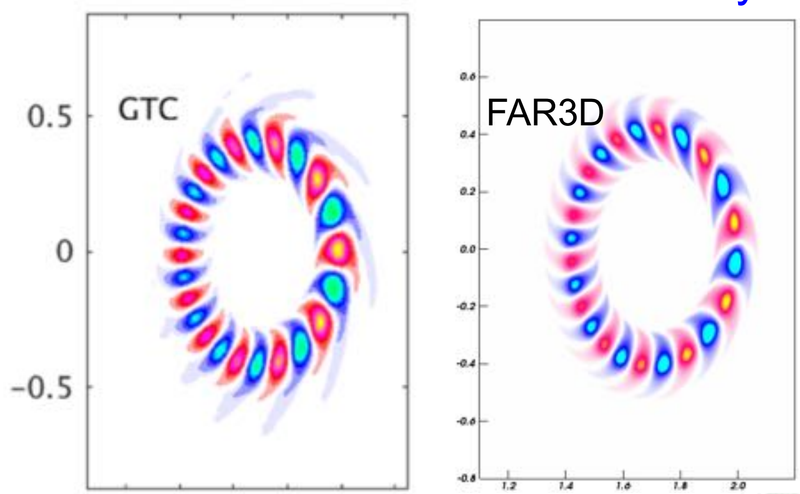

OAK RIDGE National Laboratory

Gyrofluid Equations couple reduced MHD with Hammet-Perkins closure relations

Reduced MHD equations (assumes small β, ε, $k_{\parallel}/k_{\perp}$)

Ohm's + Faraday's law: $E_{\parallel} = -\frac{\partial A_{\parallel}}{\partial t} - \hat{b} \bullet \vec{\nabla}\phi = \eta J_{\parallel}$

Toroidal component of vorticity:

$$\hat{e}_{\zeta} \bullet \vec{\nabla} \times \sqrt{g}\left\{\rho_m\left(\frac{\partial \vec{\mathrm{v}}}{\partial t} + \vec{\mathrm{v}} \bullet \vec{\nabla}\right) = -\vec{\nabla}\left(p_{th} + n_{fast}T_{fast}\right) + \vec{J} \times \vec{B}\right\}$$

Pressure evolution:

$$\frac{\partial p_{th}}{\partial t} + \vec{\mathrm{v}} \bullet \vec{\nabla} p_{th} = -\Gamma p_{th} \vec{\nabla} \bullet \vec{\mathrm{v}}$$

Basic fast ion Landau closure equations:

$$\frac{\partial n_f}{\partial t} = -\Omega_d\left(n_f\right) - n_{f0}\nabla_{\parallel}\left(\mathrm{v}_{\parallel f}\right) - n_{f0}\Omega_d\left(\frac{q_f\phi}{kT_{f0}}\right) + n_{f0}\Omega_*\left(\frac{q_f\phi}{kT_{f0}}\right)$$

$$\frac{\partial \mathrm{v}_{\parallel f}}{\partial t} = -\Omega_d\left(\mathrm{v}_{\parallel f}\right) - \left(\frac{\pi}{2}\right)^{1/2}\sqrt{\frac{kT_{f0}}{M_f}}\left|\nabla_{\parallel}\right|\left(\mathrm{v}_{\parallel f}\right) - \frac{kT_{f0}}{M_f n_{f0}}\nabla_{\parallel}\left(n_f\right) + \frac{q_f}{M_f}\Omega_*\left(\frac{\psi}{R}\right)$$

where $\Omega_d(\ ) = \frac{T_{f0}}{q_f B_0}\frac{\vec{B}_0 \times \vec{\nabla} B_0}{B_0^2} \bullet \vec{\nabla}(\ )$ and $\Omega_*(\ ) = \frac{T_{f0}}{q_f B_0 n_{f0}}\vec{\nabla} n_{f0} \bullet \frac{\vec{B}_0}{B_0} \times \vec{\nabla}(\ )$

OAK RIDGE
National Laboratory

Gyrofluid Equations couple reduced MHD with Hammet-Perkins closure relations

Reduced MHD equations (assumes small β, ε, $k_{\parallel}/k_{\perp}$)

Ohm's + Faraday's law: $E_{\parallel} = -\dfrac{\partial A_{\parallel}}{\partial t} - \hat{b}\bullet\vec{\nabla}\phi = \eta J_{\parallel}$

Toroidal component of vorticity:

$$\hat{e}_{\zeta}\bullet\vec{\nabla}\times\sqrt{g}\left\{\rho_m\left(\frac{\partial \vec{\mathrm{v}}}{\partial t}+\vec{\mathrm{v}}\bullet\vec{\nabla}\right)=-\vec{\nabla}\left(p_{th}+n_{fast}T_{fast}\right)+\vec{J}\times\vec{B}\right\}$$

Pressure evolution:

$$\frac{\partial p_{th}}{\partial t}+\vec{\mathrm{v}}\bullet\vec{\nabla}p_{th}=-\Gamma p_{th}\vec{\nabla}\bullet\vec{\mathrm{v}}$$

Basic fast ion Landau closure equations:

$$\frac{\partial n_f}{\partial t}=-\Omega_d\left(n_f\right)-n_{f0}\nabla_{\parallel}\left(\mathrm{v}_{\parallel f}\right)-n_{f0}\Omega_d\left(\frac{q_f\phi}{kT_{f0}}\right)+n_{f0}\Omega_*\left(\frac{q_f\phi}{kT_{f0}}\right)$$

$$\frac{\partial \mathrm{v}_{\parallel f}}{\partial t}=-\Omega_d\left(\mathrm{v}_{\parallel f}\right)-\left(\frac{\pi}{2}\right)^{1/2}\sqrt{\frac{kT_{f0}}{M_f}}\left|\nabla_{\parallel}\right|\left(\mathrm{v}_{\parallel f}\right)-\frac{kT_{f0}}{M_f n_{f0}}\nabla_{\parallel}\left(n_f\right)+\frac{q_f}{M_f}\Omega_*\left(\frac{\psi}{R}\right)$$

where $\Omega_d(\ )=\dfrac{T_{f0}}{q_f B_0}\dfrac{\vec{B}_0\times\vec{\nabla}B_0}{B_0^2}\bullet\vec{\nabla}(\ )$ and $\Omega_*(\ )=\dfrac{T_{f0}}{q_f B_0 n_{f0}}\vec{\nabla}n_{f0}\bullet\dfrac{\vec{B}_0}{B_0}\times\vec{\nabla}(\ )$

Recent upgrades (collaboration with Jacobo Varela, Luis Garcia):

- Thermal ion and EP FLR effects added
- Multiple fast ion species
- Two fluid (ion/electron) thermal plasma
- 3 and 4 field EP model
- Nonlinear terms

OAK RIDGE National Laboratory

Application to LHD

- J. Varela, D. Spong, L. Garcia, Nuclear Fusion (2017)
- TAE modes + MHD interchange/ballooning, parameter scans, eigenmode structures

Growth rate contours vs. S and β_{fast}

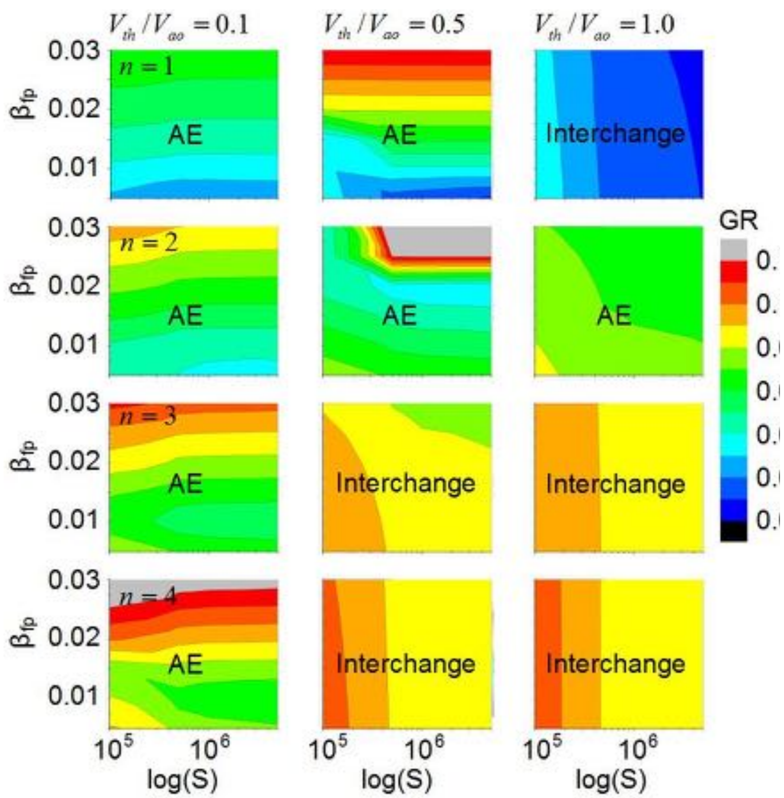

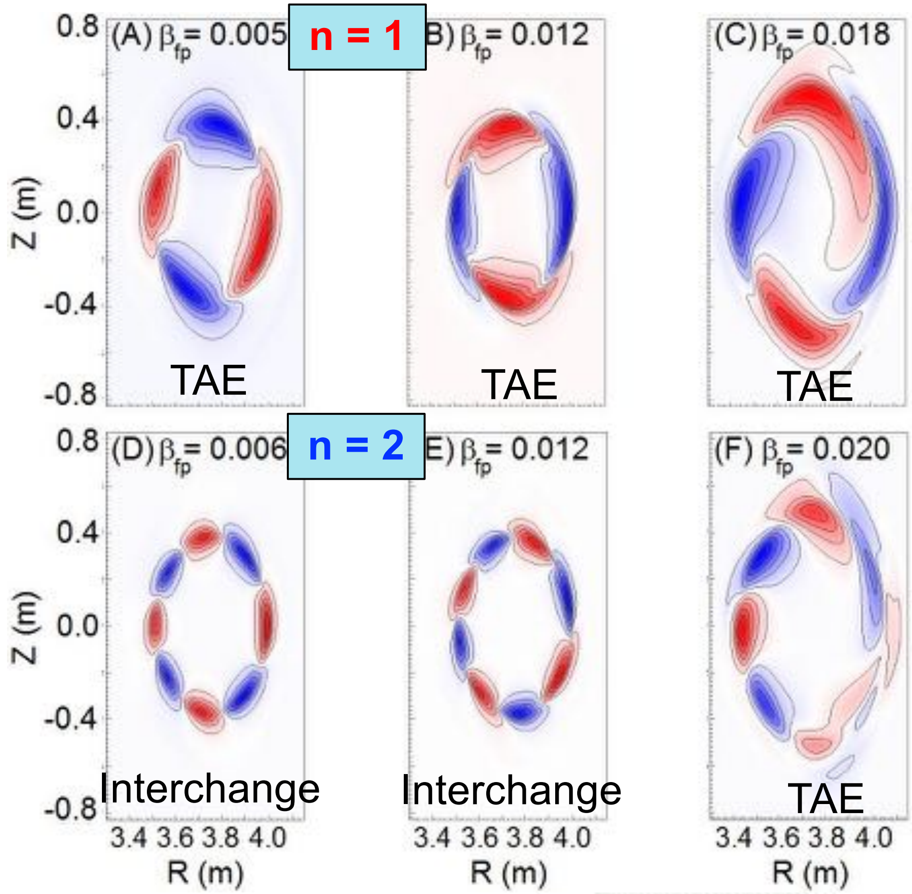

Oak Ridge National Laboratory

Application to TJ-II

J. Varela, D. Spong, L. Garcia, Nuc. Fusion (2018) Mostly helical Alfvén eigenmodes (HAE), parameter scans, eigenmode structures

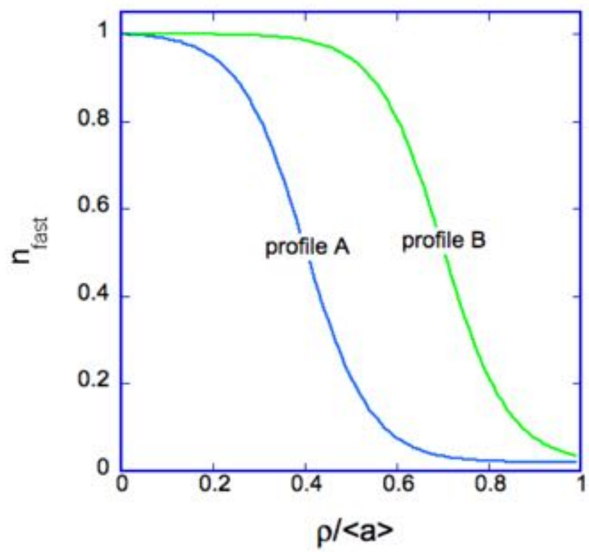

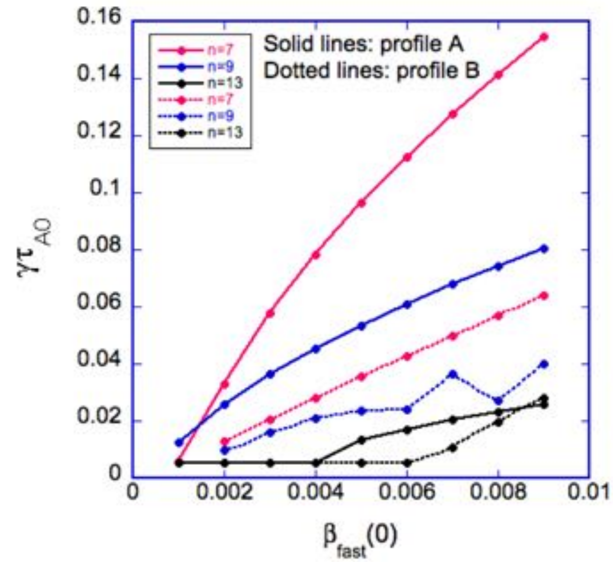

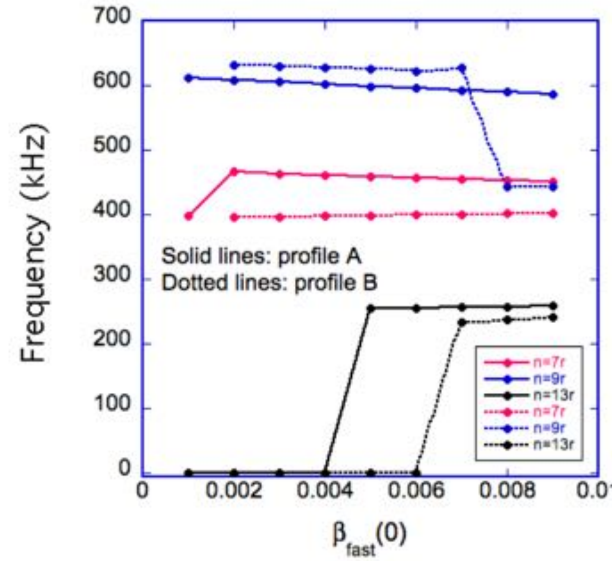

Profile A

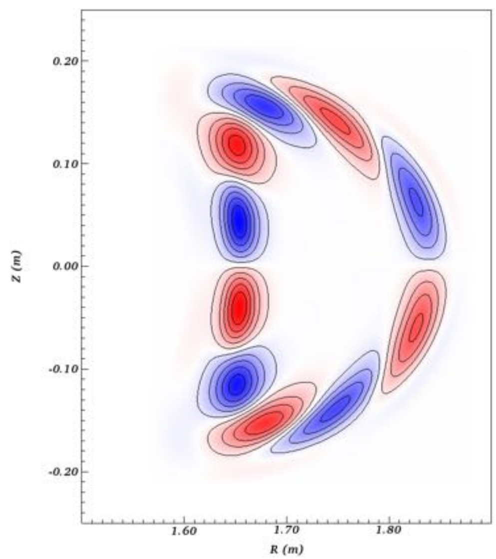

Profile B

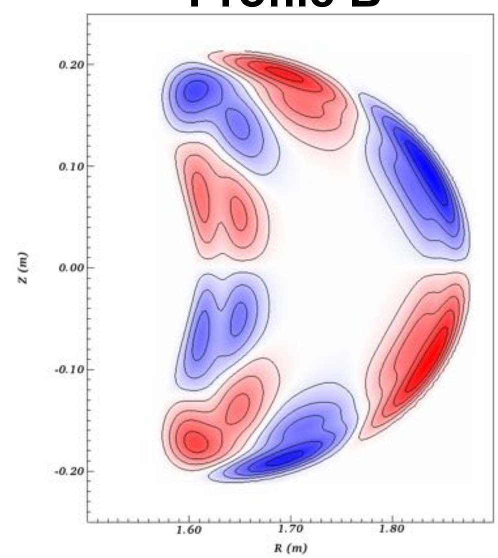

OAK RIDGE
National Laboratory

TJ-II shows many examples of dynamical frequency sweeping as the iota profile is changed:

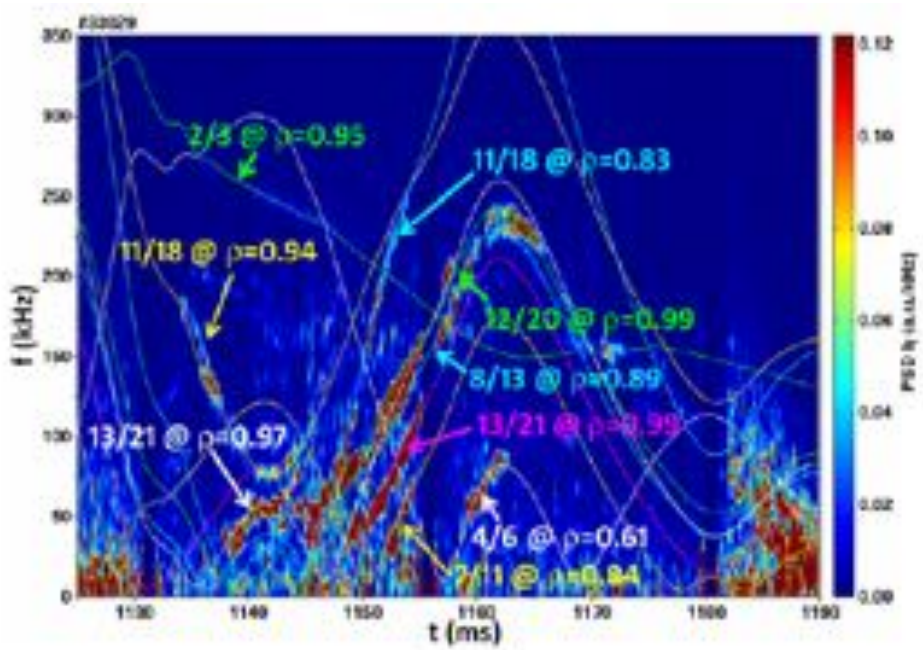

A. V. Melnikov et al, NF **54**, 123002, 2014.

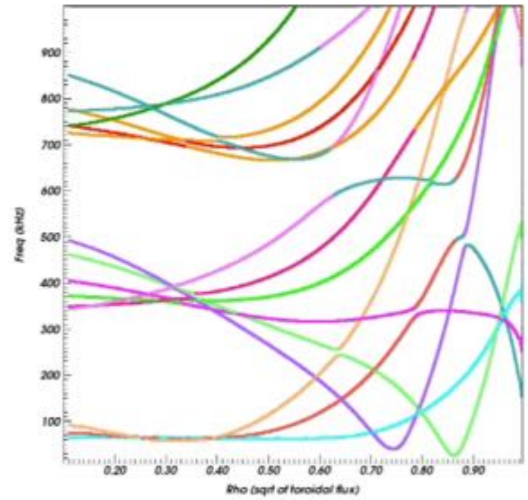

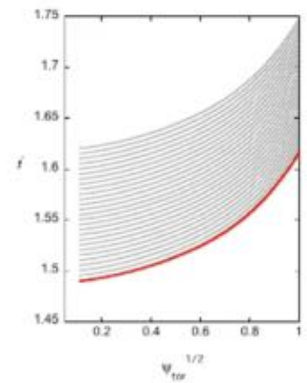

OAK RIDGE National Laboratory

Gyrofluid model reproduces TJ-II frequency sweeping effects as iota profiles are displaced

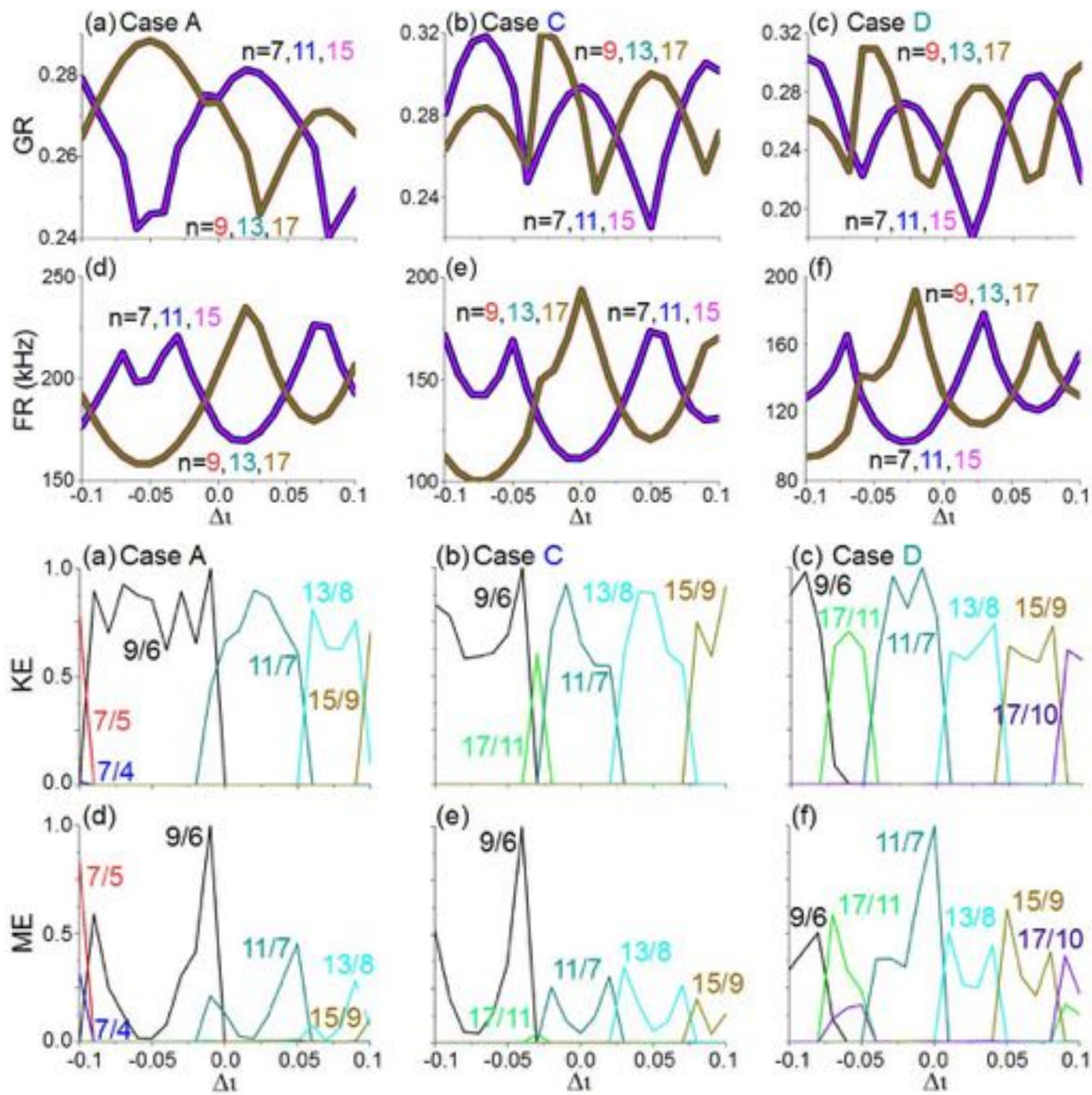

- Iota variations cause frequency sweeping, showing inverse correlations between growth rates and frequency.
- As iota changes and the frequency sweeps, different helicities become dominant

OAK RIDGE National Laboratory

NSTX Alfvén mode suppression correlated with 3D coils

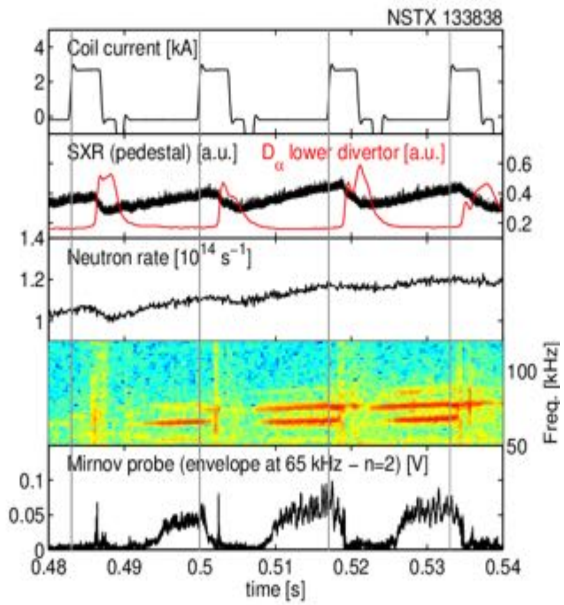

- A. Bortolon, PRL (2013), EPS (2014)
- ELMs triggered 2 ms after MP starts
- Two dominant TAEs observed
  - n=2, 65 kHz; n=3, 75 kHz
- 3D Alfvén continuum (STELLGAP model) shows toroidal coupling effects near edge => increased damping for TAE

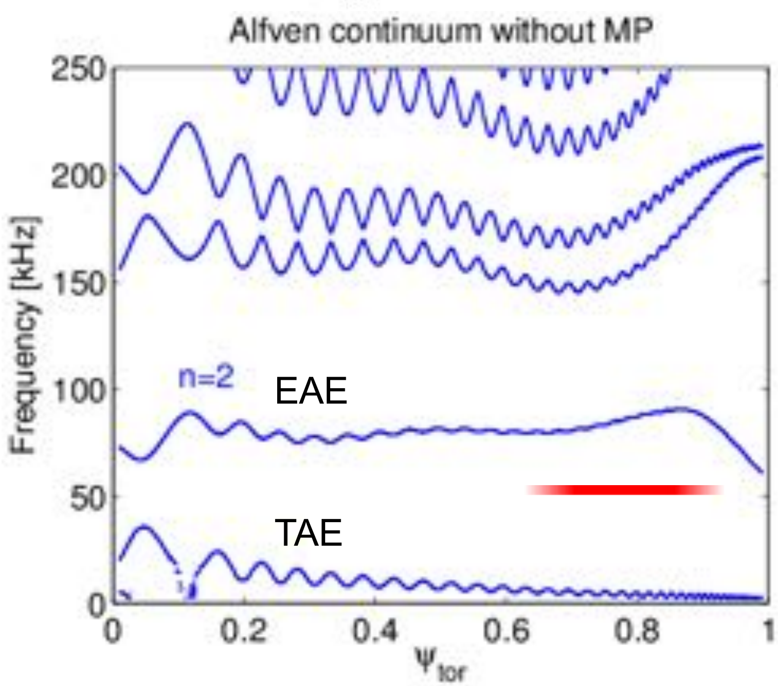

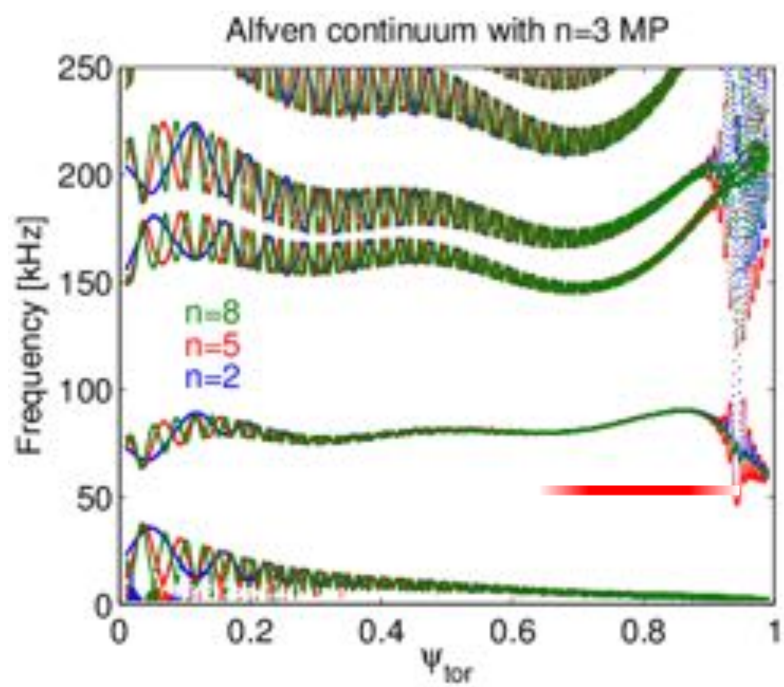

Control of EP-driven modes in stellarators

- **AE control in existing devices:**
  - Rotational transform control, ECH deposition
  - High density operation (shorter $\tau_{slow\text{-}down}$, smaller β_{EP})
- **3D shaping optimization for future designs**
  - AE gap width and locations determined by variation in $g^{\rho\rho}$, $|B|$ and ι
  - Suppress or enhance?
  - Could try to make $g^{\rho\rho}/B^2$ uniform on surface to reduce gap width
  - Target more uniform density of eigenstates vs. frequency => close off open gaps

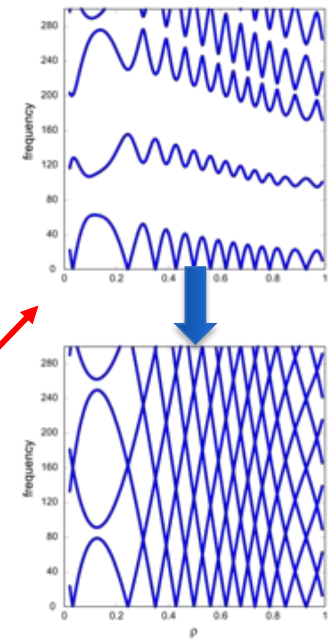

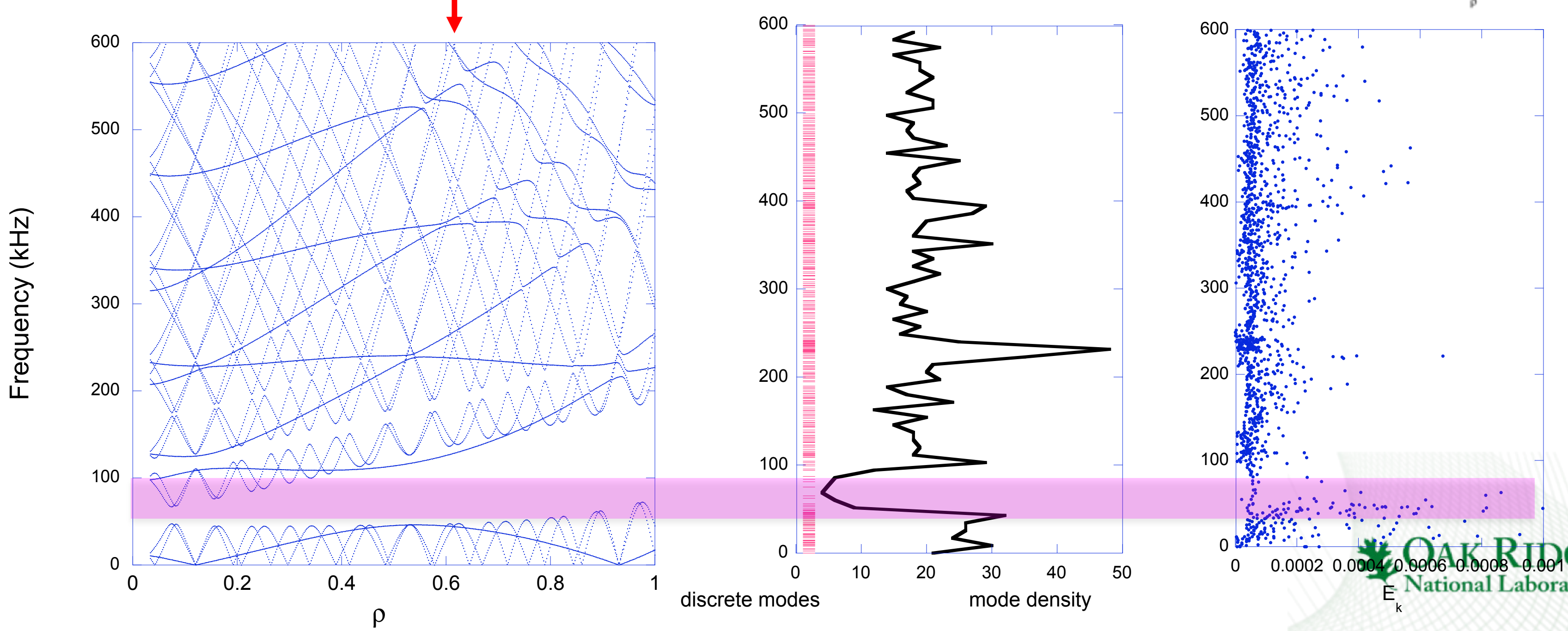

OAK RIDGE
National Laboratory

Conclusions/Summary

- Energetic particle (EP) confinement remains an important stellarator optimization goal
  - Reactor-grade confinement: stellarators still have some “catching up” to get to tokamak levels
  - Fusion power balance probably okay, PFC loading not
- EP confinement different, depending on optimization approach
  - Helically, toroidally, poloidally closed contours of |B|, QO-improvements
    - Long vs. short trapped particle bounce orbits
    - Focused vs. diffuse loss patterns
  - Innovations needed: better optimization, or ways to deal with EP losses (divertors for EP, liquid metal walls, etc.)
- A variety of EP instability models have been developed and provide understanding of EP observations
  - Stable Alfvén gap, mode structure and frequency spectra
  - Gyrokinetic, gyrofluid, particle-mode energy transfer
- EP stability optimization tools (ECH, ECCD, iota control, direct optimization) available => more tests needed